The Electrodynamic Origin of Black Holes
Part 2

Author: Raul Fattore
University Degree in Electronics Engineering

The Electrodynamic Origin of Black Holes
Part 2

Raul Fattore
https://physics-answers.com/
infobb20@gmail.com

July 7, 2026

This study is divided into two parts – Index of Part 2

Summary of Part 2

The study proves that particle fusion is the electrodynamic origin of black holes, as demonstrated by the universal electrodynamic total energy equation. It also shows that a single universal energy-curve shape appears across particle fusion, black body radiation, and binding energy per nucleon, presenting this as evidence of a universal pattern. It is demonstrated that the same framework overturns key parts of relativity by stating that particle velocity at the Schwarzschild radius is not limited to the speed of light and that black holes do not contain a mathematical "singularity" but instead a tiny, ultra-dense single atom with a mass about 0.1% of the black hole's mass, extreme energy, and near-zero temperature. The paper further presents calculations for particle types and energies inside and outside black holes, along with derived gravitational redshift equations that include motion variables absent from relativity. It is also demonstrated that Hawking radiation occurs deep inside the black hole's nucleus rather than at the Schwarzschild radius and that cosmic background radiation can be explained as electromagnetic waves of gravitational origin, matching observed microwave-to-infrared spectra in agreement with measurements from the COBE NASA satellite. The study asserts that the newly derived universal gravitational force is the only law capable of explaining "astrophysical jets" around black holes, as well as particle capture and escape.

Acronyms, Abbreviations, Keywords:
BH / BHs*: black hole / black holes*
SR*: Schwarzschild radius*
EMW: electromagnetic wave
EMR: electromagnetic radiation
EMF*:* electromagnetic field
COMU: center of mass of the universe
GEMW / GEMWs: gravitational electromagnetic wave / gravitational electromagnetic waves

Abstract

The electrodynamic origin of black holes as well as the electrodynamic origin of the gravitational force developed in the present study will contribute to a better understanding of how our universe works and obeys the real-world physics demonstrated by the more than proven laws of electrodynamics.

There are many scientific articles published on black holes. Unfortunately, almost all of them lack a real-world physics approach because authors based their studies on the pseudo-physics, invalid, and faulty theory of relativity that hindered and damaged the progress of physics for more than 100 years due to the unthinking adherence of scientists to that theory.

This study presents a new perspective that will clarify and demystify many aspects about the origin of the gravitational force through a newly derived equation with terms that are absent in basic Newton's gravitational law. It will also be demonstrated the decay of the gravitational force, the origin of black holes, what they really are, how they are formed, how they evolve, the real radiation spectrum, what particles are the constituents of black holes, what particles are to be found outside a black hole, the wavelength shift (or redshift) of black holes, and other properties.

- Do “receding” galaxies really mean that the universe is expanding?
- Is it scientifically serious to accept that gravity is not a force, but a “geometrical effect” caused by mass?
- Is it scientifically serious to accept that “geometrical gravity” lacks a unique unit of calculation, because it depends on what is being calculated?
- Can it be scientifically acceptable that a lump of Newtonian mass bends EM radiation?
- Can monochromatic radiation emission from black holes be scientifically acceptable?
- Can it be scientifically acceptable that some types of black holes do not rotate?

Based on realistic and proven universal laws of electrodynamics, the answers to these questions will naturally emerge as the current real-world study is developed.

Introduction

To gain deeper insight into the electrodynamic origin of black holes and gravitational force, the reader should be aware of some important flaws of the theory of relativity. A theory that contributed to the misinformation about how Mother Nature works.

The theory of relativity violates its basis, i.e., the tenet of relative motion. **Relative motion depends on relative coordinates, not on reference frames** [1]. Magnitudes measured from a **relational motion** will have the same value on **any** frame of reference. Also, the theory postulates the equivalence of inertial mass with gravitational mass. According to this theory, gravity is not a force but a curvature of space-time, i.e., a geometrical property, so that **the gravitational mass is not subject to Newton's third law**. An absolute contradiction to the mass equivalence principle.

The **velocity of light is not absolute,** as postulated in the theory of relativity. The velocity of light depends on the relative motion between sources or between the source and detector (observer). **The velocity of an EMW is only constant relative to the medium**. The velocity of light obeys the principle of relative velocity addition/subtraction so that **there is no speed limit in the universe**. The velocity of an EMW source adds/subtracts to the wavefront speed. Otherwise, no Doppler effect or Cherenkov effect can be observed.

Another important flaw in the theory of relativity is a **wrong energy equation** that only depends on velocity while the acceleration of the system is not taken into account. This is especially dangerous when applied to nuclear fusion, where massive acceleration of charges exists. It means that **radiation energy calculation is totally ignored** [2]. The momentum change equation in the theory of relativity is also flawed because it lacks an acceleration term as well.

The absence of a real-world physical explanation of the “unusual” high velocity in the outer arms of spiral galaxies gave rise to the unphysical and absurd assertion that it is caused by "dark matter" or "dark energy." How scientists could accept something like that is beyond understanding.

The present study is based on the **universal electrodynamic force** [3], from which the new gravitational law is derived. Also from the universal force, a **universal total energy** equation has been derived [4]. **This is the first time in physics a true total energy equation has been formulated**, including the classical potential energy term and **kinetic energy terms depending on velocity and acceleration**. A universal total momentum change equation with an acceleration term has also been derived from the universal force. These equations have been successfully applied to calculate the real released energy in nuclear fusion and the real energy of the products, as well as the discrete atomic energy levels and atomic spectra [5].

The cosmic-scale application of the universal electrodynamic force, energy, and momentum equations will be demonstrated throughout this study.

The universal electrodynamic equations are valid on any scale, from subatomic particles to cosmic dimensions.

The Electrodynamic Origin of Black Holes

The scientific literature in general differentiates between a quasar and a black hole. However, they are one and the same thing. The origin of black holes arises naturally from energy analysis for particle fusion made with the universal electrodynamic total energy equation.

The universal electrodynamic total energy equation

For the first time in physics, **a true total energy equation** has been formulated, including terms accounting for potential energy **and kinetic energy depending not only on velocity but also acceleration**.

The Universal Total Energy [4] is derived from the Universal Electrodynamic Force, which gives us an accurate energy equation. You can find more details in the article *Nuclear Fusion Enhanced by Negative Mass – A Proposed Method and Device – (Part 2)*.

The Total Energy equation has three terms:

1) The ***Potential Energy term***, which depends on the relative position of the charges.

2) One ***Kinetic Energy term***, which depends on the relative **velocity** of the charges.

3) One ***Kinetic Energy term***, which depends on the relative **acceleration** of the charges. This term accounts for **radiation energy** and is not found in scientific literature as being part of the total energy of the system.

$$E = \frac{1}{\sqrt{1+(\cos(\theta)^2-1)\frac{v^2}{c^2}}}\left(kq_1q_2\left(\frac{1}{r_f}-\frac{1}{r_i}\right)-\frac{kq_1q_2}{c^2}\left(\frac{1}{r_f}-\frac{1}{r_i}\right)v^2+\frac{2kq_1q_2\cos(\alpha)}{c^2}\left(\ln(r_i)-\ln(r_f)\right)a\right) \quad (16)$$

The initial distance is usually taken such that the rest energy of the system is approximately zero, which usually means $r=\infty$. But as infinity is not a defined number, let's take a practical value from Mother Nature that can realistically be used instead. Infinity can be replaced by a huge distance, approx. x10 bigger than the oldest light we have observed from the "Big Bang" ($46500\ 10^6 ly = 4.4 10^{26} m$). To be safe, we'll take $r_i = 10^{27} m$.

However, **zero energy does not just happen when charges are at rest and separated by large distances**. As demonstrated in the article "Nuclear Fusion Enhanced by Negative Mass - A Proposed Method and Device (Part 2)," **there is a second solution to Eq. (16)** that, depending on the system dynamics, **yields zero energy for a specific close distance**.

For the first time in physics, it has been found that **zero energy is impacted not just by potential energy but also by the system's dynamics**.

As we can see in Eq. (16), the total energy is affected by a factor $\gamma_E = \frac{1}{\sqrt{1+(\cos^2(\theta)-1)\frac{v^2}{c^2}}}$ that is physically realistic compared to the known "Lorentz factor" because it also takes into account the type of motion that is given by the angle θ between $\vec{r}$ and $\vec{v}$ (the relative position and velocity). Note that the "Lorentz factor" is only valid for circular motion. Also note that $1 \leq \gamma_E \leq \infty$ depending on the angle θ between $\vec{r}$ and $\vec{v}$ **and** the relative velocity, reaching a maximum value (or ∞) for $\theta = \frac{\pi}{2}$.

We can write the **total energy** of the system in short form as:

$$E = \gamma_E(U + K + E_{rad}) \qquad (17)$$

The "rest energy" is no other than the potential energy "U" when the kinetic variables are zero ($v = 0$ **and** $a = 0$). The Universal Force shows us that zero velocity doesn't mean that acceleration should be zero. Note that in this case $\gamma_E = 1$. Under such conditions, the rest energy is:

$E = E_0 = U$

The "rest energy" depends on the distance between the centers of charges, the kinetic energy term *K* depends on the relative velocity, and the kinetic energy term due to acceleration (radiation energy) is E_{rad}.

We successfully applied the Total Energy equation, among other things, to precisely calculate **the real released energy** in nuclear fusion and the single energy of the products, **including radiation energy**. For more details, read the section "*How to Calculate the Real Released Energy and the Single Energy of the Products*" in the article *Nuclear Fusion Enhanced by Negative Mass – A Proposed Method and Device – (Part 3)*.

Equation (16) can be used to calculate EMR absorption or emission indistinctly. It is merely a sign change due to the angle α (head-on motion or the opposite).

The Universal Shape of the Curve of Energy

The universal force and universal total energy equations show us that the force and energy curve have a universal shape. The same pattern can be seen in particle fusion, nuclei fusion, binding energy per nucleon, nuclei density, black-body radiation, gravitational energy, celestial bodies' density, etc.

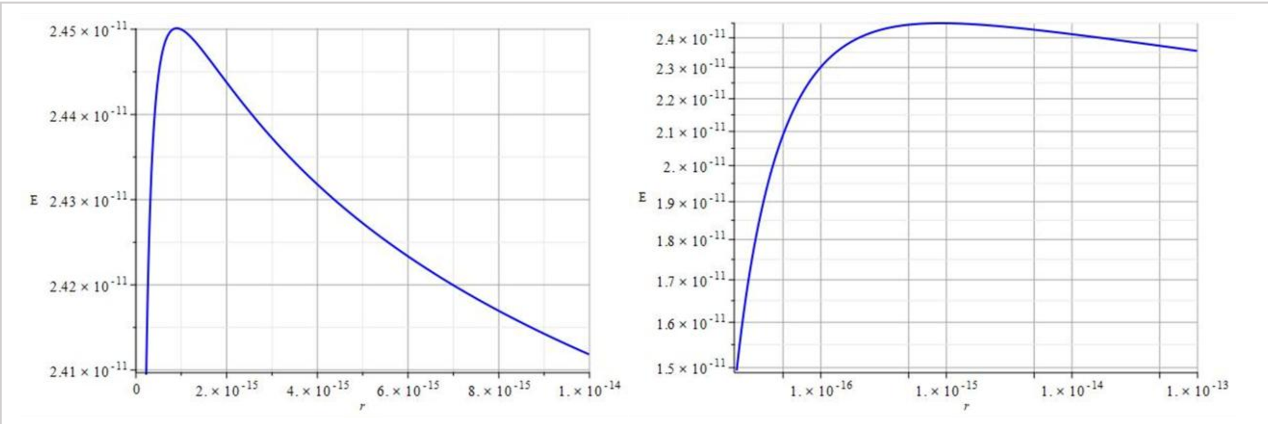

Figure 6
Left: energy graph in regular scale – Right: energy graph in logarithmic scale
Universal shape of the energy curve from the interaction electron-proton

In Fig. 6 we see an example of the energy curve for the electron-proton head-on interaction in both regular scale and logarithmic scale.

Another example is the curve of the binding energy per nucleon. In general, the number of protons in nuclei is equal to the number of neutrons, except for a few nuclei that have more neutrons than protons. For simplicity, let's assume that all nuclei have an equal number of protons and neutrons. As the neutron is a proton-electron bound, nuclei will always have double the number of protons than electrons, which are organized in alternating nuclear “sandwich” shells as described in this article. Then, we can replace the charges in Eq. (16) as $q_1 = 2\, q_p$ and $q_2 = q_e$.

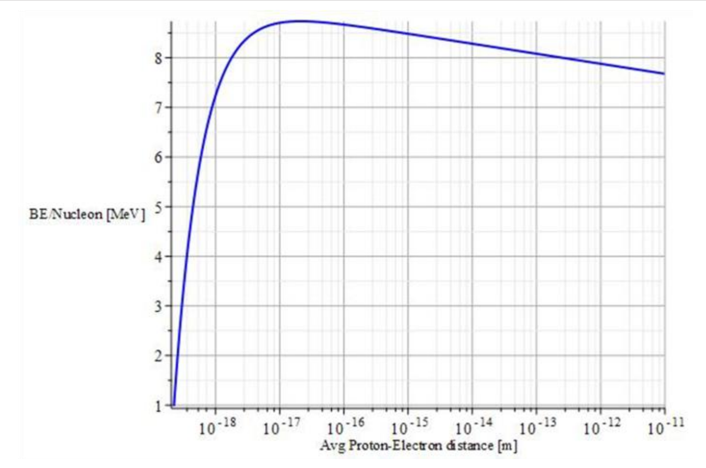

Figure 7
Binding energy per nucleon determined by the electrodynamic total energy equation

The binding energy per nucleon is the energy divided by the mass number: $E_n = \frac{E}{A}$.

We assume head-on motion ($\alpha = \theta = \pi$) and take the element with the highest number of protons which is Oganesson, with Z=118, A=294, N=176.

To get the energy in eV, the energy equation is multiplied by the proper factor. The curve of binding energy per nucleon shown in Fig. 7 was obtained for $a = 4.4\ 10^{32}\ [\frac{m}{s^2}]$ and $v = 2.7\ 10^{8}\ [\frac{m}{s}]$.

As we can see, there is no more need for empirical formulas to find the binding energy per nucleon.

The couple of examples given above are only the tip of the iceberg to show you the extent of the universal total energy. As demonstrated in the study on the new atomic model, the total energy equation also provides precise calculations of the energy of particles and atomic energy levels as well as the spectral lines from energy absorption or emission from elements.

Particle Fusion as the Origin of Black Holes Proved with the Universal Total Energy Equation

In the article Nuclear Fusion Enhanced by Negative Mass – A Proposed Method and Device – (Part 2), we have already analyzed the points of **maximum force, zero force, maximum energy, and zero energy** for the special case of **proton-proton fusion**, i.e., head-on motion ($\alpha = \theta = \pi$).

Now we'll do a general analysis and find the point of maximum energy given by Eq. (16) by taking the derivative with respect to r equal to zero.

$$\frac{\partial}{\partial r}(E) = 0 = \gamma_E\left(-\frac{kq_1q_2}{r^2} + \frac{kq_1q_2v^2}{c^2r^2} - \frac{2kq_1q_2\cos(\alpha)a}{c^2r}\right) = 0$$

Solving for r:

$$r = -\frac{c^2\left(1-\frac{v^2}{c^2}\right)}{2\cos(\alpha)a} \qquad (18)$$

This is the distance for the maximum energy and zero force, while the maximum force happens at double this distance.

Now assume that the magnitude of the acceleration is caused by a mass M located at the distance r:

$a = \frac{G\,M}{r^2}$ (19)

Replacing (19) in (18) and solving for r, we get two solutions:

$r = 0$; however, as particles have a real physical radius, this is just an unphysical mathematical solution that will be dismissed. So, the only remaining possibility is to take the second solution:

$$r = -\frac{2\cos(\alpha)GM}{c^2\left(1-\frac{v^2}{c^2}\right)} \quad (20)$$

Equation (20) is the **general expression of the Schwarzschild radius** (SR) that we may identify as $r_s = -\frac{2\cos(\alpha)GM}{c^2\left(1-\frac{v^2}{c^2}\right)}$ (21)

In the special case of head-on motion ($\alpha = \pi$) for $v << c$, the SR reduces to the following:

$$r_s = \frac{2\,G\,M}{c^2} \quad (22)$$

The real "**accretion radius" (2 SR)** arises naturally when finding **the point of maximum force**, which is double the Schwarzschild radius: $r_{acc} = 2\,r_s$. See Figs. 9 and 10.

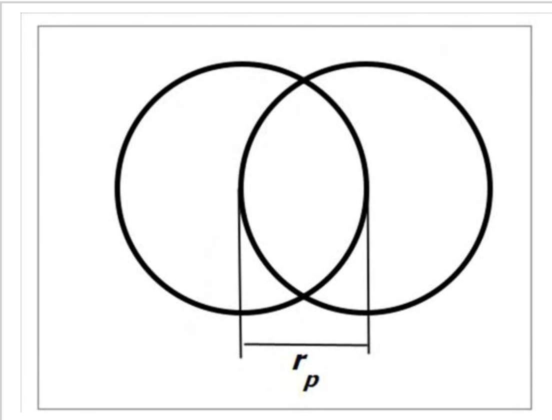

Figure 8
Fusion of two protons. The Schwarzschild radius is the radius of the particle during the fusion process.

In the article Nuclear Fusion Enhanced by Negative Mass – A Proposed Method and Device – (Part 1) we have demonstrated that the Schwarzschild radius is exactly the radius of the particles at the moment they fuse, i.e., when the particles overlap by their radii, as shown in Fig. 8 for the proton-proton fusion.

As stated before, this is the point of **maximum energy and zero force**.

Equation (18) tells us that at the particle scale the SR does not depend on the charges but entirely on the kinetics of the system given by the relative velocity **and** acceleration.

The Lennard-Jones Potential model as well as the Van der Waals interactions, Van der Waals force, and Van der Waals radius are not based on the laws of Electrodynamics.

The interaction distance between single charges, nuclei, atoms, or molecules is dynamic and depends on the kinetics of the system. Thus, assigning fixed values of "Van der Waals radii" to the elements in the periodic table is completely wrong.

Though at a large scale the lump Newtonian mass appears in the equation of the SR, there is no critical mass or mass limit for the formation of a black hole, which is caused by particle fusion. The Chandrasekhar limit does not play any role in the formation of black holes.

The Tolman–Oppenheimer–Volkoff limit is invalid. Moreover, those equations totally ignore the energy that is given by the kinetics of the system, which is responsible for the SR. This is indeed not a black hole but "a hole" in the theory of relativity that demonstrates a very poor physical assessment of the problem.

Magnitudes and Range of the Schwarzschild Radius, Velocity, and Acceleration
Equation (18) is the general equation of the Schwarzschild radius that proves the electrodynamic origin of black holes. As r is a magnitude and to have a defined positive value $0 < r < \infty$ means that the acceleration must always be greater than zero $a > 0$, while the velocity will have two ranges depending on the type of motion.

To simplify, let's assume two scenarios where particles move in the same line in opposite directions ($\alpha = \pi$, head-on motion) or in the same direction ($\alpha = 0$, away motion). In both cases $\alpha = \theta$, and $\gamma_E = 1$. Therefore, the positive sign for our solution will reduce to the following two cases:

1) If $\alpha = \theta = \pi$ (head-on motion), then the velocity must be $v < c$.

2) If $\alpha = \theta = 0$ (away motion), then the velocity must be $v > c$.

The second case could be applied to media where the Cherenkov effect is observable.

Magnitude of the SR and its range

1) *For head-on motion* ($\alpha = \theta = \pi$): $r = \frac{c^2\left(1-\frac{v^2}{c^2}\right)}{2a}$. If $v = 0$, then $r = \frac{c^2}{2a}$. If $v < c$, then $r < \frac{c^2}{2a}$.

As the acceleration can never be infinite or zero for r to exist, it means that the SR will always have a minimum and maximum value, so that its range for this motion is $0 < r \leq \frac{c^2}{2a}$.

2) *For away motion* ($\alpha = \theta = 0$): $r = -\frac{c^2\left(1-\frac{v^2}{c^2}\right)}{2a}$. There is no valid solution for $0 \leq v < c$. If $v > c$, then $r > \frac{c^2}{2a}$. Thus, the SR range for this motion is $r > \frac{c^2}{2a}$.

Magnitude of the velocity and its range

When solving Eq. (18) for the velocity, we get: $v = c\sqrt{1 + \frac{2ra\cos(\alpha)}{c^2}}$.

1) *For head-on motion* ($\alpha = \theta = \pi$): $v = c\sqrt{1 - \frac{2ar}{c^2}}$. A real solution requires that $a \leq \frac{c^2}{2r}$. Since a can never be zero, its range is: $0 < a \leq \frac{c^2}{2r}$. If $a = \frac{c^2}{2r}$, then $v = 0$. If $0 < a < \frac{c^2}{2r}$, then $v < c$. Thus, the velocity range for this motion is $0 \leq v < c$.

2) *For away motion* ($\alpha = \theta = 0$): $v = c\sqrt{1 + \frac{2ar}{c^2}}$. If $a = \frac{c^2}{2r}$, then $v = \sqrt{2}\,c$. If $0 < a < \frac{c^2}{2r}$, then $v < \sqrt{2}\,c$. If $a > \frac{c^2}{2r}$, then $v > \sqrt{2}\,c$. Therefore, for this motion the relative velocity range will be $v > c$, depending on the relative acceleration. For very low acceleration, the relative velocity may have a minimum magnitude $v \approx c$.

Magnitude of the acceleration and its range

When solving Eq. (18) for the acceleration, we get: $a = -\frac{c^2\left(1-\frac{v^2}{c^2}\right)}{2\cos(\alpha)r}$.

1) *For head-on motion* ($\alpha = \theta = \pi$): $a = \frac{c^2\left(1-\frac{v^2}{c^2}\right)}{2r}$. As *a* can never be zero, we have seen that the velocity range for head-on motion is $0 \leq v < c$. For $v = 0$, then $a = \frac{c^2}{2r}$. For $0 < v < c$, then $a < \frac{c^2}{2r}$. Thus, the acceleration range for head-on motion is $0 < a < \frac{c^2}{2r}$.

2) *For away motion* ($\alpha = \theta = 0$): $a = -\frac{c^2\left(1-\frac{v^2}{c^2}\right)}{2r}$. As the magnitude of *a* must be always positive and greater than zero, the minimum relative velocity for away motion must be $v > c$, so that $a > \frac{c^2}{2r}$. The maximum relative velocity for away motion is $v = \sqrt{2}\,c$, that makes $a = \frac{c^2}{2r}$. So, the acceleration range for away motion is $a \geq \frac{c^2}{2r}$.

Summarizing the magnitudes of the relative motion variables at the SR and their range, according to the type of motion

Magnitudes of the relative motion variables at the SR and their range						
Variables	*Head-on motion* ($\alpha = \theta = \pi$)			*Away motion* ($\alpha = \theta = 0$)		
	At the SR		*Range*	*At the SR*		*Range*
r	$\frac{c^2}{2a}$	$< \frac{c^2}{2a}$	$0 < r \leq \frac{c^2}{2a}$	$\frac{c^2}{2a}$	$> \frac{c^2}{2a}$	$r \geq \frac{c^2}{2a}$
v	0	$< c$	$0 \leq v < c$	$\sqrt{2}\,c$	$> c$	$v > c$
a	$\frac{c^2}{2r}$	$0 < a < \frac{c^2}{2r}$	$0 < a \leq \frac{c^2}{2r}$	$\frac{c^2}{2r}$	$> \frac{c^2}{2r}$	$a \geq \frac{c^2}{2r}$

Figure 8a
Table summarizing the magnitudes of the relative motion variables at the SR and their range, according to the type of motion

In Fig. 8a we have summarized all the calculations from the previous sections for the motion variables according to two types of motion.

The relative velocity $v = c$ commonly assigned to the SR is just a mathematical limit that makes the equation of the SR undefined.

It is not a physically realistic velocity magnitude to be adopted in the real world for the SR.

The zero relative velocity in head-on motion means the moment of impact or fusion of the colliding particles at the SR. This is also confirmed by the zero momentum change at that point (see Fig. 9).

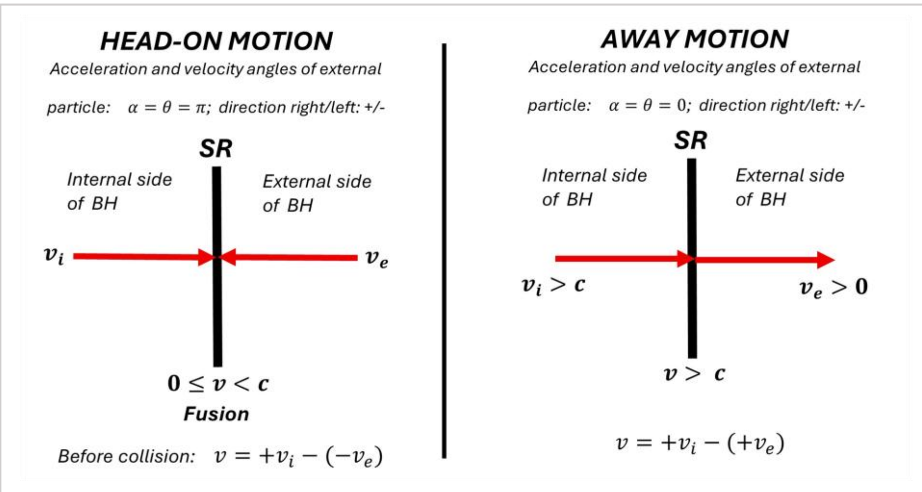

Figure 8b
Relative velocity for particles at the limits of the Schwarzschild radius. Head-on motion and away motion of particles in black holes

As shown in Fig. 8b, at the internal limit of the SR, particles are moving with velocity $v_i < c$ **for head-on motion**.

However, **for away motion,** the internal velocity must be $v_i > c$ for an external particle to have $v_e > c$ in the right direction.

It's important to know that $v_i = 0$ near the SR does not happen.

We see that for an internal particle to get outside the BH, it needs a velocity $v_i > c$.

That may happen depending on the refractive index around the SR region (Cherenkov effect).

The Nucleus of a Black Hole

We have stated before that the universal total energy equation (16) has **two solutions for zero energy**: one given by the **potential energy** (at a very large distance) and the other (at a very short distance) given by the **kinetics of the system**, i.e., velocity **and** acceleration.

Thus, for the first time in physics, we cannot assume anymore that zero energy only happens when the particles are separated by very large distances.

This is an extremely important consequence that will define a small black hole region that we call a **nucleus**, where particles are trapped.

Within the nucleus, energy absorption is always much greater than energy release. We'll see later that **there is a very tiny region within the nucleus with an approximate radius of $r \approx 10^{-60}$ $[m]$ where no radiation takes place but only energy absorption**. As the nuclear radius increases, radiation energy also increases from very faint to relevant magnitudes.

As a picture is worth a thousand words, let's summarize all of the above with a couple of pictures that will show the physics behind a black hole formation, as well as what particles and radiation we may expect outside and within a black hole in general. In a later section we'll analyze in detail black holes of several sizes and prove that **the radiation described by Hawking does not happen at the SR** [16] but deep inside in BHs, within the nuclear region. Therefore, it cannot be measured.

In Fig. 9 we see an example of the electrodynamic origin of black holes and how a black hole originates from an electron-proton fusion. The curves of force, energy, and momentum are very clear in describing the physical effect. It is obvious that a massive black hole will never be created from the isolated fusion of two or even a small bunch of particles. The BH created by the fusion of a few particles will not be maintained and will immediately be "evaporated" by radiation loss.

A massive black hole could be formed from the extensive and almost simultaneous fusion of a monumental number of particles caused by a cosmic cataclysm like a gigantic explosion of a cosmic object.

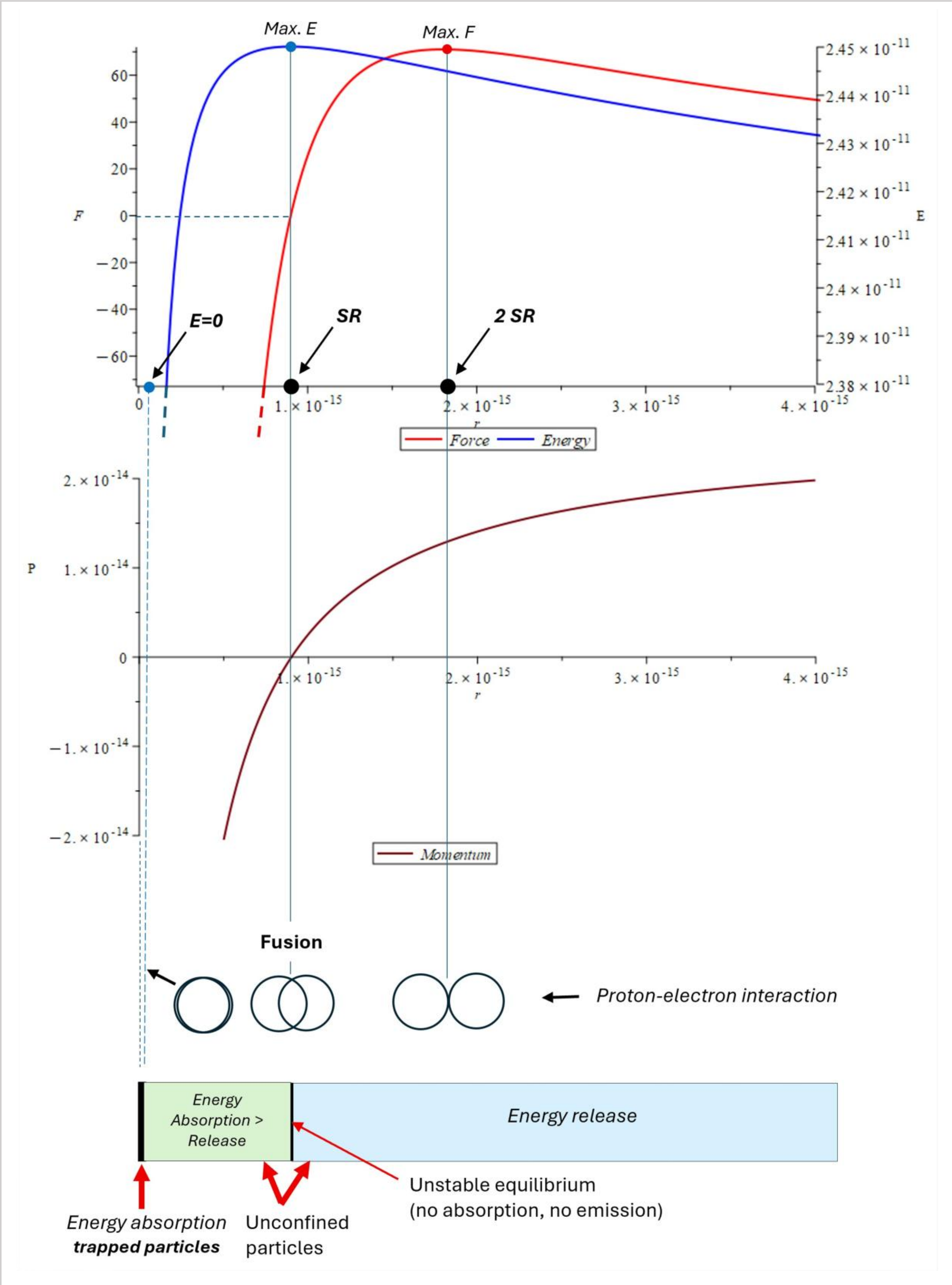

Figure 9

Example of black hole formation during electron-proton fusion – Graph of force, energy, and momentum

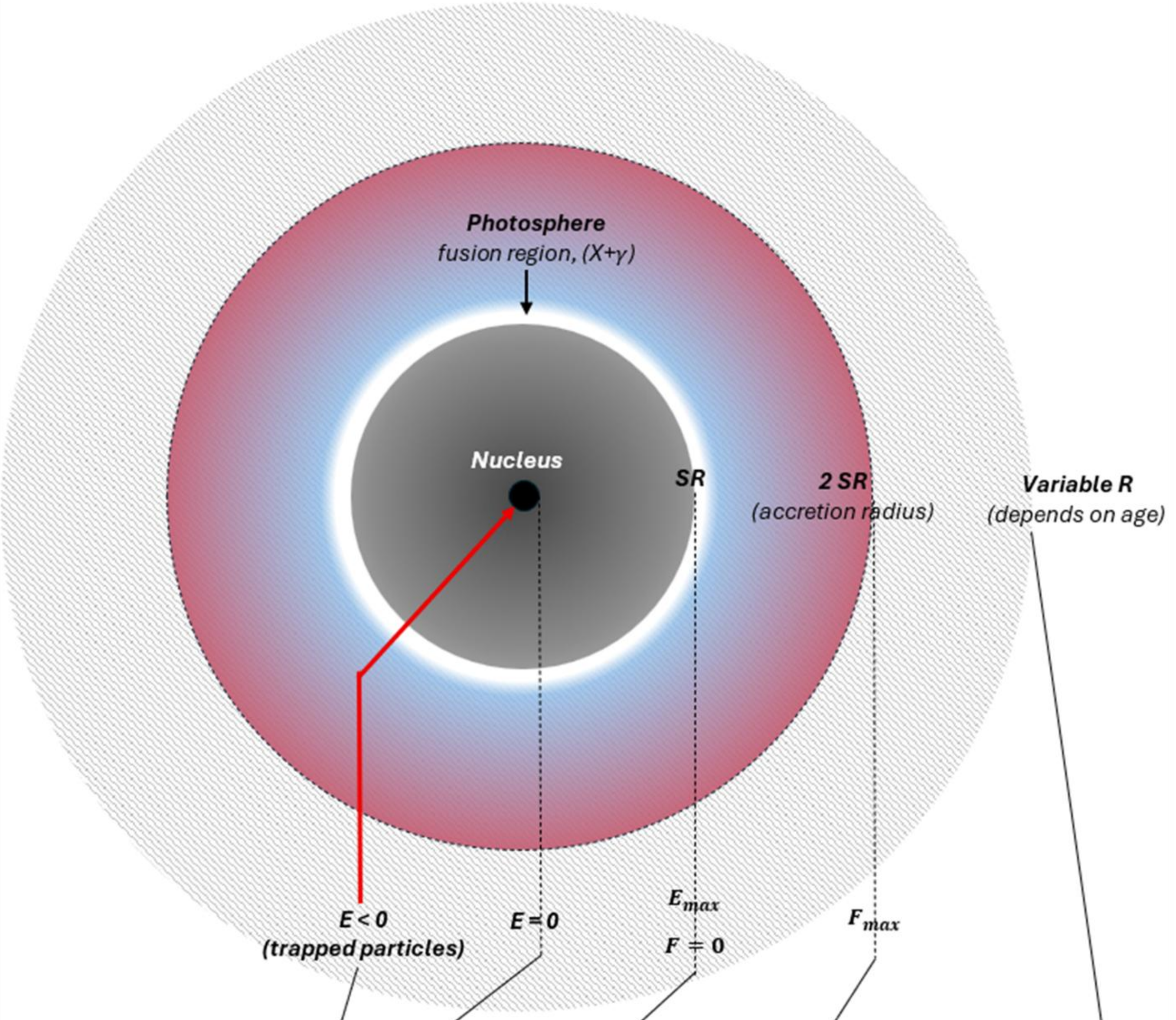

New Electromagnetic Theory of Elementary Particles	***Atoms*** (1 toroidal helix)	Particles with 2 toroidal helices	Particles with 3 or more toroidal helices	Several proton and electron toroidal helices organized in nuclei surrounded by stable positioned electrons, all balanced by EM forces
Standard Model of Elementary Particles	$d, \bar{d}$	$\nu_e, \bar{\nu}_e, \pi^0(type\ 1),$ $u, \bar{u},$	$e^-, e^+, p, \bar{p}, \nu_e, \bar{\nu}_e,$ $n, \bar{n}, s, \bar{s},$ $\pi^-, \pi^+, \pi^0(type\ 2),$ $\nu_\mu, \bar{\nu}_\mu, c, \bar{c}, b, \bar{b},$ $t, \bar{t}, \nu_\tau, \bar{\nu}_\tau$	***Atoms*** H, He, O.., Fe, Ni, Au, Pt, Ag, U... *(depends on age)*
Energy	Absorption >> faint to high release	Absorption > Release	Release	
Radiation	None + very faint Radio + Microwave	Microwave + IR + Radio	Microwave + IR + UV + $(X + \gamma)$	Radio + Microwave + IR + UV + $(X + \gamma)$
Particles' state	Trapped	Unconfined		

Figure 10
Example of a black hole with its nucleus, constituent particles, and radiation

The Energy of the Particles

We see in Fig. 10 that not all particles are trapped inside the SR. Trapped particles are confined only in a tiny region inside the BH, which we call the **nucleus**. It is also shown the types of particles according to the New Electromagnetic Theory of Elementary Particles, and the approximately equivalent particles for the Standard Model of Elementary Particles.

It is recommended to read the article New Atomic Model with Real-Valued Wave Function – Energy Levels, Spectrum, and Atomic Fine Structure for a better understanding of the type of particles we may find inside a BH, their size, and energy levels.

You should bear in mind that particles are elastic. Thus, their size changes according to the environment. **No particles can be given an invariant size**. Protons and electrons within a neutron will have a very small radius (high energy) as they do when they are outside the neutron. Electrons in the proximity of an element nucleus will have a smaller radius (more energy) compared with those in peripheric shells (less energy). **A shift in size means a change in energy.**

As demonstrated by Bostick [15] and also in the new atomic model article [5], particles have a finite size as defined by a toroidal charge fiber helix, and their energy is given by:

$$E = \frac{kq^2}{\pi r_0} \ln\left(\frac{r_0}{r_h}\right) \quad (23)$$

Where k is the Coulomb constant, q is the particle charge, r_0 is the particle radius (torus radius), and r_h is the charge fiber helix radius.

Types of Particles in a Black Hole

Elementary particles are usually composed of various intertwined helices, while the real atom consists of only one charge fiber helix [5]. Thus, the radii ratio changes accordingly so that the energy equation of the particle will be different depending on if its location is within or outside the black hole, as follows:

a) *Elementary particles composed of three or more charge fibers* ($q = \pm e$) **are found outside the BH** and are the cause of fusion at the Schwarzschild radius:

$$E = \frac{kq^2}{\pi r_0} \ln(10^{186}) \quad (24)$$

b) *Elementary particles composed of two charge fibers* ($q = \pm \frac{2}{3} e$) **are located within the black hole, between the internal limit of the SR and the external limit of the nucleus**:

$$E = \frac{kq^2}{\pi r_0} \ln(1.6\ 10^{421}) \quad (25a)$$

c) ***Atoms***, *which are elementary particles composed of one charge fiber* ($q = \pm \frac{1}{3} e$) **are located within the nucleus**. There is no such thing as a mathematical "singularity" at the center of a black hole. Note that **at the center of the nucleus, we find only one atom** whose mass is about 0.1% the mass of the BH. The energy equation for the particles (atoms) in the nucleus is:

$$E = \frac{kq^2}{\pi r_0} \cdot \ln(3.24\ 10^{1687}) \quad (25b)$$

Gravitational Force and Acceleration of a Particle Within a Black Hole

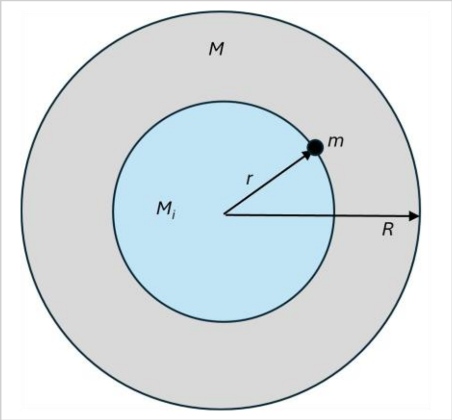

Figure 11
Gravitational force and acceleration on a mass m within a black hole

A black hole is not a hole at all nor an empty body. It is a massive cosmic object composed of a high density of particles. Therefore, there is no different physics than that used in other celestial bodies to find the gravitational force on a little mass within the BH.

Let's analyze the force and acceleration on a particle of mass *m* at a radius *r* caused by the gravitational force of a BH assumed spherical, with average (constant) density ρ, mass M, and radius R. Note that $R = r_s$.

As shown in Fig. 11, a concentric sphere of mass M_i is contained in M. The mass of the inner sphere is the effective mass that causes the gravitational force on *m*.

The new universal gravitational force in geometrical form given in Eq. (9) applied to this case is:

$$\vec{F}_G = -\frac{G\,m\,M_i}{r^2}\left(\left(1 - \frac{45}{8}\beta^2 \cos(\theta)^2\right)\hat{r} + \frac{45}{8}\beta\cos(\theta)\,\vec{\beta}\right) \quad (26)$$

Where: $\beta = \frac{v}{c}$, $\vec{\beta} = \frac{\vec{v}}{c}$, and θ is the angle between $\vec{r}$ and $\vec{v}$. We can write $\vec{v} = v\,\hat{r}$ and make the replacements on Eq. (26) considering that the attractive motion is radial, i.e., $\theta = \pi$. After some algebra, we get:

$$F_G = -\frac{G\,m\,M_i}{r^2}\left(1 - \frac{45}{4}\frac{v^2}{c^2}\right)\hat{r} \quad (27)$$

However, as mass *m* is on the surface shell of mass M_i, the relative velocity between both masses is zero, and the equation reduces to:

$$F_G = -\frac{G\,m\,M_i}{r^2}\hat{r} \quad (28)$$

Where $M_i = \frac{4}{3}\pi\,r^3\rho$ (29)

Replacing (29) in (28): $F_G = -\frac{Gm\frac{4}{3}\pi r^3\rho}{r^2}\hat{r}$ (30)

Now, the density of the BH is $\rho = \frac{M}{V} = \frac{M}{\frac{4}{3}\pi\,r_s^3}$. After replacing the SR from Eq. (22), we have:

$$\rho = \frac{3\,c^6}{32\,\pi\,M^2\,G^3} \quad (31)$$

Replacing (31) in (30): $F_G = -\frac{\frac{1}{8}m\,r\,c^6}{G^2\,M^2}\hat{r}$ (32). The mass of the BH is: $M = \frac{Rc^2}{2G}$ (33), where $R = r_s$.

Replacing (33) in (32), we finally obtain the equation of the gravitational force on mass *m* at a radius *r* within the BH:

$$F_G = -\frac{1}{2}m\,c^2\frac{r}{R^2}\hat{r} \quad (34)$$

This force varies linearly with *r* and is valid up to $r = R$. Applying Newton's second law:

$-\frac{1}{2}m\,c^2\frac{r}{R^2}\hat{r} = -m\,a\,\hat{r}$, so that the gravitational acceleration on the particle of mass *m* is:

$$a = \frac{1}{2}c^2\frac{r}{R^2} \quad (35)$$

This equation is valid within the BH, up to $r = R$. In fact, for $r = R$, we obtain the same expression of the acceleration as when it is derived from the SR equation: $a = \frac{c^4}{4GM}$.

Velocity of a Particle Within a Black Hole Caused by the Gravitational Acceleration

Particles within the black hole will have some degree of motion (vibration) that greatly reduces as we move to the center of the BH, where the velocity will be zero. We see from Eq. (35) that the acceleration depends on the position of the particle. Thus, we can write:

$$a = \frac{dv}{dt}\frac{dr}{dr} \;\Rightarrow\; a = v\frac{dv}{dr} \;\Rightarrow\; v\,dv = a\,dr \qquad (36)$$

Now we can integrate (36):

$$\int_{v_0}^{v} v\,dv = \int_{R_0}^{r} a\,dr \qquad (37)$$

Where R_0 is **the minimum radius of the black hole**, equivalent to the **atom radius** at the center of the BH, and v_0 is its velocity, which is indeed zero, while v is the velocity of the particle at a radius r.

There is no unphysical “singularity” at the center of a black hole. There will be **only one atom** (toroidal charge fiber helix) with extremely tiny dimensions but not zero. In further sections we’ll see that the energy of this atom is extremely high but not infinite, while its equivalent mass is around 0.1% the mass of the black hole.

By replacing (35) in (37), we proceed with the integration of (37) and solve for v, which will give the velocity of the particle caused by the gravitational acceleration of the BH at a radius *r*:

$$v = \frac{\sqrt{2}}{2}c\sqrt{\left(1 - \frac{R_0^2}{r^2}\right)\frac{r}{R}} \qquad (38)$$

This equation is valid within the BH up to $r = R$.

The **minimum velocity**, as expected, is found at the center of the BH when $r = R_0$, that is $v_{min} = 0$. The **maximum velocity** takes place at the SR, when $r = R$:

$$v_{max} = \frac{\sqrt{2}}{2}c \qquad (39)$$

We see that the particle **at the inner limit** of the SR never reaches $v = c$.

Energy of a Particle Within a Black Hole Caused by the Gravitational Acceleration

In previous sections we described the total energy of a system of charges that is specified by Eq. (16). To analyze the interaction between a black hole and a particle, we’ll replace one of the charges by the mass of the BH. The mass of a particle can be written as:

$$m = \frac{kq^2}{r_0\,c^2}[Kg] \qquad (40)$$

Where k is the Coulomb constant and r_0 the radius of the charge.

We’ll assume head-on motion ($\alpha = \theta = \pi$), so that our total energy Eq. (16) becomes:

$$E = kq_1q_2\left(\left(\frac{1}{r} - \frac{1}{10^{27}}\right) - \frac{1}{c^2}\left(\frac{1}{r} - \frac{1}{10^{27}}\right)v^2 - \frac{2}{c^2}(\ln(10^{27}) - \ln(r))a\right) \qquad (41)$$

The gravitational force is attractive, so we should define the interaction between positive and negative charges. So, let's name the negative charge $q_1 = q$, and write q_2 in terms of the BH mass, assuming that $q_2 = q_p$ is a positive charge.

The total number of charges contained in the mass *M* of the BH can be defined as $N\, q_p$. As only single particles can be assumed in the BH, then the atomic number Z doesn't play any role in the total number of charges. Multiplying and dividing the total number of charges by $k\, q_2\, r_0\, c^2$:

$$N\, q_p\, \frac{k\, q_p\, r_0\, c^2}{k\, q_p\, r_0\, c^2} = \frac{k\, N\, q_p^2}{r_0\, c^2}\, \frac{r_0\, c^2}{k\, q_p} = M\, \frac{r_0\, c^2}{k\, q_p} \qquad (42)$$

Equation (42) will replace q_2 in (41), while q will be the other charge:

$$E = k\, q\, M\, \frac{r_0\, c^2}{k\, q_p}\left(\left(\frac{1}{r} - \frac{1}{10^{27}}\right) - \frac{1}{c^2}\left(\frac{1}{r} - \frac{1}{10^{27}}\right) v^2 - \frac{2}{c^2}\left(ln(10^{27}) - ln(r)\right) a\right) \qquad (43)$$

The magnitude of the total energy given by Eq. (43) combined with Eqs. (24), (25a), and (25b) will be later applied to calculate the size, energy, and radiation of a particle in the black hole.

Particle Dimensions at the Schwarzschild Radius, at the Center, and at Different Radii Within a Black Hole

The electrodynamic origin of black holes tells us that a black hole cannot be assumed to be a perfect isolated black body in thermal equilibrium, where the temperature is the same on its surface as at any point inside.

The radii of the particles will change within the BH, according to its radius; thus, particle radiation energy will be different at different depths.

To make calculations, we'll find the radiation energy at different depths of a BH and use the Stefan-Boltzmann law to get the result of the radiation temperature and wavelength as follows:

a) *On the whole surface area* of the BH, as if those radiations were measured on the SR

b) *On the equivalent shell surface for a certain radius* within the BH

In all cases the energy of the particle that is given by Eqs. (24), (25a), or (25b) must be equal to the magnitude of the total energy Eq. (43).

Particle Dimension at the Schwarzschild Radius

In this case we'll assume the interaction between an electron ($q = -e$), and the BH of mass M having the positive charge of a proton ($q_p = +e$). By equating Eq. (24) with the magnitude of the energy given by Eq. (43), we solve for the particle radius r_0:

$$k\, q\, M\, \frac{r_0\, c^2}{k\, q_p}\left(\left(\frac{1}{r} - \frac{1}{10^{27}}\right) - \frac{1}{c^2}\left(\frac{1}{r} - \frac{1}{10^{27}}\right) v^2 - \frac{2}{c^2}\left(ln(10^{27}) - ln(r)\right) a\right) = \frac{kq^2}{\pi r_0}\ln(10^{186}) \qquad (44)$$

Velocity at the SR ($r = \frac{2GM}{c^2}$) will be set to zero, and the acceleration set to $a = \frac{GM}{r^2}$. We'll see that the particle size at the SR is practically the same for all black holes.

See Figures 14 to 18 for results calculated for various black holes.

Particle Radius at the Center of a Black Hole

We have previously stated that there is no mathematical "singularity" at the center of a BH, but a single atom with a finite size. In this case the radius of the particle (atom) will be coincident with the radius of the black hole in that position.

The central atom has a charge of $q = -\frac{e}{3}$, which will interact with surrounding charges $q_p = +\frac{e}{3}$. The velocity according to Eq. (38) will be zero, and the acceleration will be given by Eq. (35). Equating the energy Eq. (25b) with the magnitude of the energy given by Eq. (43), we solve for the particle radius r_0 at the center of the black hole for $r = r_0$.

$$k\ q\ M\ \frac{r_0\, c^2}{k\ q_p}\left(\left(\frac{1}{r}-\frac{1}{10^{27}}\right)-\frac{1}{c^2}\left(\frac{1}{r}-\frac{1}{10^{27}}\right)v^2-\frac{2}{c^2}\left(ln(10^{27})-ln(r)\right)a\right)=\frac{kq^2}{\pi r_0}\cdot\ln(3.24\ 10^{1687}) \quad (45)$$

See Figures 14 to 18 for results calculated for various black holes.

Particle Radius at Different Depths Within a Black Hole

Here we have to differentiate two regions:

a) *Within the nucleus*

b) *Outside the nucleus, up to the internal limit of the Schwarzschild radius*

Within the nucleus we have the interaction of charges $q = -\frac{e}{3}$ and $q_p = +\frac{e}{3}$. Equation (45) is valid for calculations at any radius r within the whole nucleus.

Outside the nucleus, the interaction will be for charges $q = -\frac{2\,e}{3}$ and $q_p = +\frac{2\,e}{3}$. Equating the energy Eq. (25a) with the magnitude of the energy given by Eq. (43), we solve for the particle radius r_0 for BH radii r between the internal limit of the SR and the external limit of the nucleus.

$$k\ q\ M\ \frac{r_0\, c^2}{k\ q_p}\left(\left(\frac{1}{r}-\frac{1}{10^{27}}\right)-\frac{1}{c^2}\left(\frac{1}{r}-\frac{1}{10^{27}}\right)v^2-\frac{2}{c^2}\left(ln(10^{27})-ln(r)\right)a\right)=\frac{kq^2}{\pi r_0}\ln(1.6\ 10^{421}) \quad (46)$$

Velocity will be given by Eq. (38) and acceleration by Eq. (35).

See Figures 14 to 18 for results calculated for various black holes.

Pressure on Particle Within a Black Hole

In previous paragraphs we have calculated the gravitational force exerted by the black hole on a particle of mass *m* located within the BH, which is given by Eq. (34). Following our new atomic model, the particle structure is an elastic toroidal charge fiber helix having a torus radius r_0, a helix radius r_h, and a fiber radius approximately $r_F = \frac{r_h}{10}$, while its charge depends on the number of fibers and their organization, though this is irrelevant in pressure calculations.

Due to the tiny dimension of the particle when interacting with a BH, we can approximate the surface area of the toroidal charge fiber helix to:

$$S = (2\pi r_0)\cdot(2\pi r_F) \quad (47)$$

Where r_0 is the particle radius (torus radius) and r_F is the toroidal helix fiber radius.

The pressure $P = \frac{F_G}{S}$ (48) will be calculated at diverse positions in the BH, according to the type of particle.

Energy equations (24), (25a), and (25b) show that the ratio between particle radius and helix radius $\frac{r_0}{r_h}$ changes according to the position of the particle within the BH.

a) **For particles in the nucleus**: $\frac{r_0}{r_h} = 3.24\ 10^{1687}$, and $r_F = \frac{r_0}{3.24\ 10^{1688}}$. After making replacements in Eq. (48), the pressure equation in the nucleus will be: $P = \frac{4.1\ 10^{1686} m\, c^2 r}{R^2 r_0^2}$ (49).

b) **For particles outside the nucleus** up to the internal limit of the SR: $\frac{r_0}{r_h} = 1.6\ 10^{421}$, and $r_F = \frac{r_0}{1.6\ 10^{422}}$. After making replacements in Eq. (48), the pressure equation outside the nucleus will be: $P = \frac{2\ 10^{420} m\, c^2 r}{R^2 r_0^2}$ (50)

c) **For particles at the SR**: $\frac{r_0}{r_h} = 10^{186}$, and $r_F = \frac{r_0}{10^{187}}$. After making replacements in Eq. (48), the pressure equation at the SR will be: $P = \frac{1.27\ 10^{185} m\, c^2 r}{R^2 r_0^2}$ (51).

See Figures 14 to 18 for results calculated for various black holes.

Radius of the Nucleus for Black Holes of $\mathbf{1\ M_\odot}$, $\mathbf{10^2\ M_\odot}$, $\mathbf{10^4 M_\odot}$, $\mathbf{10^6 M_\odot}$ and $\mathbf{10^{11} M_\odot}$

As we have declared before when analyzing the **universal total energy** given by Eq. (16), there are two solutions for zero energy: one at a very large distance that depends mainly on the potential energy term and the other at a shorter distance, which depends on the system dynamics.

To determine the radius of the nucleus of a black hole, we take the velocity at the internal limit of the Schwarzschild radius, which is $v_{max} = \frac{\sqrt{2}}{2} c$ as given by Eq. (39), and the acceleration $a = \frac{c^4}{4GM}$ as given by Eq. (35).

By equating the energy Eq. (43) to zero and solving for *r*, we'll get two distance solutions, where the smallest is the radius of the nucleus:

$$E = k\ q\ M\ \frac{r_0\, c^2}{k\ q_p}\left(\left(\frac{1}{r} - \frac{1}{10^{27}}\right) - \frac{1}{c^2}\left(\frac{1}{r} - \frac{1}{10^{27}}\right) v^2 - \frac{2}{c^2}\left(ln(10^{27}) - ln(r)\right) a\right) = 0 \quad (52)$$

In Fig. 12 the size of the nucleus is shown for diverse BH masses.

BH Mass	$1 M_\odot$	$10^2\ M_\odot$	$10^4\ M_\odot$	$10^6\ M_\odot$	$10^{11}\ M_\odot$
SR [m]	$2.966\ 10^3$	$2.966\ 10^5$	$2.966\ 10^7$	$2.966\ 10^9$	$2.966\ 10^{14}$
Radius of the Nucleus r_n [m]	25	$2.7\ 10^3$	$3\ 10^5$	$3.3\ 10^7$	$4.5\ 10^{12}$

Figure 12

Radius of the nucleus for diverse black hole masses

Determining the Radiation of a Black Hole

Our **universal total energy** Eq. (16), from which we found the electrodynamic origin of black holes, can be written in short form as $E = \gamma_E(U + K + E_{rad})$. In our analysis of BHs for head-on motion of particles $\gamma_E = 1$, so that $E = U + K + E_{rad}$, where U is the potential energy, K is the kinetic energy due to velocity, and E_{rad} is the kinetic energy due to acceleration, which is the radiation energy. Thus, the total energy and its individual terms are:

$$E = k\,q\,M\,\frac{r_0\,c^2}{k\,q_p}\left(\left(\frac{1}{r}-\frac{1}{r_i}\right)-\frac{1}{c^2}\left(\frac{1}{r}-\frac{1}{r_i}\right)v^2-\frac{2}{c^2}\left(ln(r_i)-ln(r)\right)a\right)$$

$$U = kqM\frac{r_0c^2}{kq_p}\left(\frac{1}{r}-\frac{1}{r_i}\right) \quad (53)$$

$$K = -kqM\frac{r_0c^2}{kq_p}\frac{1}{c^2}\left(\frac{1}{r}-\frac{1}{r_i}\right)v^2 \quad (54)$$

$$E_{rad} = -kqM\frac{r_0c^2}{kq_p}\frac{2}{c^2}\left(\ln(r_i)-\ln(r)\right)a \quad (55)$$

For most regular calculations, the initial distance is usually taken as $r_i = 10^{27}[m]$. However, to improve the accuracy of the energy results for BHs, we'll greatly increase the initial distance not to infinite but to $r_i = 10^{4260}[m]$, which will provide excellent results.

To ascertain the dynamics, we'll show the magnitude and sign of the total energy and of each of its terms. To calculate the radiating temperature and wavelength at different depths in BHs, we equate the radiation energy E_{rad} with the energy in Joules given by the Stefan-Boltzmann law:

$$E = \epsilon\,\sigma\,A\,T^4\,t = E_{rad} \quad (56)$$

Taking $t = 1[s]$ and solving Eq. (56) for T, we get the radiating temperature $T = \sqrt[4]{\frac{E_{rad}}{\epsilon\sigma A}}$ (57). Assuming $\epsilon = 1$, we obtain the wavelength from Wien's displacement law $\lambda = \frac{2.898\;10^{-3}}{\mathrm{T}}$ (58).

Equation (57) will be solved for two different surface areas:

a) *The surface area given by the Schwarzschild radius*

b) *The surface areas given by the different radii within the BH*

Note that radiation in the nucleus region will remain in the nucleus (trapped particles) because energy absorption is much greater than energy release.

Radiation outside the nucleus may or may not get outside the BH, depending on the type of motion.

Radiation at the SR is entirely due to particle fusion. Thus, the faint radiation calculated by Hawking can never be from the Schwarzschild radius [16].

Summary of Radiation and Particle Data for Various Black Hole Masses

The following figures (Fig. 14 to Fig. 18) show a summary with all calculated magnitudes as detailed in previous sections for black holes of $1\mathrm{M}_\odot$, $10^2\mathrm{M}_\odot$, $10^4\mathrm{M}_\odot$, $10^6\mathrm{M}_\odot$ and $10^{11}\mathrm{M}_\odot$.

Note that "Hawking radiation" appears deep inside the nucleus in all cases. The total energy in the nucleus is determined mainly by the potential energy, while outside the nucleus the main contribution to the total energy is due to radiation. At the SR (fusion region), the potential energy cancels out with the kinetic energy given by velocity, and the total energy is due exclusively to radiation.

The center of a BH is probably the only place in the universe where the temperature is practically zero degrees Kelvin ($T \approx 0\ [K]$) and no radiation exists. Since the nucleus of a BH is a region of trapped particles where energy absorption is much greater than energy release, the calculated radiation in that region will most probably never get outside the nucleus.

In various studies we have already demonstrated the invalidity of the ill-fated theory of relativity that arbitrarily imposed a velocity limit in the universe, which does not exist in the real world. As shown in Fig. 8a, the relative velocity can be greater than the speed of light, depending on the type of motion. Thus, part of the radiation from particles outside the nucleus may be measured outside the black hole.

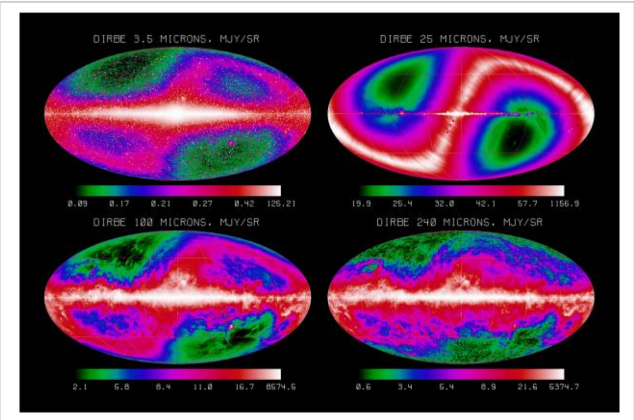

Figure 13
Cosmic Infrared Background (CIB) radiation (COBE NASA)

Note also that by taking an average BH, the calculated radiation spectrum lies approximately between microwaves and infrared, which is consistent with COBE NASA satellite measurements shown in Fig. 2 and Fig. 13.

It is a clear demonstration that the cosmic background radiation is caused by electromagnetic waves of gravitational origin.

$1\ M_{\odot}$ — *Nucleus radius 25* $[m]$															
Particles' charge $[C]$	$q=\pm\frac{e}{3}$								$q=\pm\frac{2e}{3}$						$q=\pm e$
BH inner radius $r\,[m]$	$1.76\,10^{-73}$	10^{-65}	10^{-30}	10^{-24}	10^{-10}	10^{-6}	10^{-3}	1	50	10^{2}	10^{3}	$1.5\,10^{3}$	$2.5\,10^{3}$	$2.95\,10^{3}$	**(SR)** $2.966\,10^{3}$
Particle radius $r_0\,[m]$	$1.76\,10^{-73}$	$1.3\,10^{-69}$	$4.2\,10^{-52}$	$4.2\,10^{-49}$	$4.2\,10^{-42}$	$7.2\,10^{-40}$	$2.3\,10^{-38}$	$4.2\,10^{-37}$	$6\,10^{-36}$	$4.3\,10^{-36}$	$5.7\,10^{-36}$	$4.5\,10^{-36}$	$3.4\,10^{-36}$	$3.1\,10^{-36}$	$3.1\,10^{-36}$
Particle mass $m\,[Kg]$	$1.6\,10^{27}$	$2\,10^{23}$	$6.7\,10^{5}$	$7\,10^{2}$	$7\,10^{-5}$	$7\,10^{-7}$	$2.2\,10^{-8}$	$6.7\,10^{-10}$	$4.7\,10^{-11}$	$2.6\,10^{-10}$	$2\,10^{-10}$	$2.5\,10^{-10}$	$3.3\,10^{-10}$	$3.7\,10^{-10}$	$8\,10^{-10}$
Pressure on particle $P\,[Pa]$	$4\,10^{1796}$	$5\,10^{1792}$	$1.6\,10^{1775}$	$1.6\,10^{1772}$	$1.6\,10^{1765}$	$5.6\,10^{1762}$	$1.7\,10^{1761}$	$1.6\,10^{1760}$	$1.3\,10^{492}$	$3\,10^{493}$	$1.3\,10^{494}$	$3.8\,10^{494}$	$1.5\,10^{495}$	$2.3\,10^{495}$	$3\,10^{260}$
Energy $[J]$ — **Total E**	$-9\,10^{46}$	$-2.3\,10^{43}$	$-7.5\,10^{25}$	$-7.4\,10^{22}$	$-7.5\,10^{15}$	$-7.5\,10^{13}$	$-2.3\,10^{12}$	$-7.5\,10^{10}$	$1.9\,10^{10}$	$7.8\,10^{10}$	$1.14\,10^{12}$	$1.3\,10^{12}$	$1.7\,10^{12}$	$1.8\,10^{12}$	$1.8\,10^{12}$
Energy $[J]$ — U	$-9\,10^{46}$	$-2.3\,10^{43}$	$-7.5\,10^{25}$	$-7.4\,10^{22}$	$-7.5\,10^{15}$	$-7.5\,10^{13}$	$-2.3\,10^{12}$	$-7.5\,10^{10}$	-10^{10}	$-7.7\,10^{9}$	-10^{9}	$-5.4\,10^{8}$	$-2.4\,10^{8}$	$-2\,10^{8}$	$-2\,10^{8}$
Energy $[J]$ — K	~ 0	10^{-94}	$4\,10^{-42}$	$4.2\,10^{-33}$	$4.3\,10^{-12}$	$4.3\,10^{-6}$	$1.3\,10^{-1}$	$4.3\,10^{3}$	$1.5\,10^{6}$	$4\,10^{6}$	$6\,10^{7}$	$7\,10^{7}$	$9\,10^{7}$	$9\,10^{7}$	$2\,10^{8}$
Energy $[J]$ — E_{rad}	$3\,10^{-102}$	$2.6\,10^{-90}$	$8.5\,10^{-38}$	$8.3\,10^{-29}$	$8.4\,10^{-8}$	$8.4\,10^{-2}$	$2.6\,10^{3}$	$8\,10^{7}$	$3\,10^{10}$	$8.6\,10^{10}$	$1.14\,10^{12}$	$1.3\,10^{12}$	$1.7\,10^{12}$	$1.8\,10^{12}$	$1.8\,10^{12}$
$T\,[°K]$ **@ SR** (from E_{rad})	$2.7\,10^{-26}$	$2.5\,10^{-23}$	$3\,10^{-10}$	**$6.1\,10^{-8}$ Hawking**	10^{-2}	0.3	4.5	61	$2\,10^{2}$	342	$6.5\,10^{2}$	$6.8\,10^{2}$	$7\,10^{2}$	$7.3\,10^{2}$	$7.4\,10^{2}$
$\lambda\,[m]$ **@ SR**	10^{23}	10^{20}	$8.5\,10^{6}$	$4.7\,10^{4}$	0.3	$8.5\,10^{-3}$	$0.6\,10^{-3}$	$48\,10^{-6}$	$11\,10^{-6}$	$8.5\,10^{-6}$	$4.4\,10^{-6}$	$4.2\,10^{-6}$	$4\,10^{-6}$	$3.9\,10^{-6}$	$3.9\,10^{-6}$
Spectrum	*Undefined*		*Radio (ELF to VLF)*		*Microwave*			*IR (from FIR to MIR)*							
$T\,[°K]$ **@ r** (from E_{rad})	$3.5\,10^{12}$	$4\,10^{11}$	$1.8\,10^{7}$	$3\,10^{6}$	$6\,10^{4}$	$1.8\,10^{4}$	$6.8\,10^{3}$	$3.3\,10^{3}$	$2\,10^{3}$	$1.8\,10^{3}$	10^{3}	$9.5\,10^{2}$	$7.8\,10^{2}$	$7.3\,10^{2}$	$7.3\,10^{2}$
$\lambda\,[m]$ **@ r**	$8.4\,10^{-16}$	$7\,10^{-15}$	$1.5\,10^{-10}$	$9\,10^{-10}$	$5\,10^{-8}$	$1.5\,10^{-7}$	$4.3\,10^{-7}$	$0.88\,10^{-6}$	$1.4\,10^{-6}$	$1.5\,10^{-6}$	$2.6\,10^{-6}$	$3\,10^{-6}$	$3.7\,10^{-6}$	$3.9\,10^{-6}$	$3.9\,10^{-6}$
Spectrum	γ		*X-rays*		*UV*			*IR*							

Figure 14
Radiation and particle data for a 1 solar mass black hole

$10^2\,M_\odot$ Nucleus radius $2.7\,10^3$ [m]														
Particles' charge [C]	$q=\pm\frac{e}{3}$								$q=\pm\frac{2e}{3}$					$q=\pm e$
BH inner radius r [m]	$1.76\,10^{-75}$	10^{-63}	10^{-28}	$2.2\,10^{-25}$	10^{-8}	10^{-4}	10^{-1}	10^{2}	10^{4}	10^{5}	$1.5\,10^{5}$	$2.5\,10^{5}$	$2.95\,10^{5}$	**(SR)** $2.966\,10^{5}$
Particle radius r_0 [m]	$1.76\,10^{-75}$	$2.3\,10^{-69}$	$4.2\,10^{-52}$	$1.9\,10^{-50}$	$4.2\,10^{-42}$	$4.2\,10^{-40}$	$1.3\,10^{-38}$	$4.2\,10^{-37}$	$4.3\,10^{-36}$	$6\,10^{-36}$	$4.7\,10^{-36}$	$3.5\,10^{-36}$	$3.2\,10^{-36}$	$3.2\,10^{-36}$
Particle mass m [Kg]	$1.6\,10^{29}$	$2.2\,10^{23}$	$7\,10^{5}$	$1.4\,10^{4}$	$7\,10^{-5}$	$7\,10^{-7}$	$2.2\,10^{-8}$	$7\,10^{-10}$	$2.6\,10^{-10}$	$2\,10^{-10}$	$2.4\,10^{-10}$	$3\,10^{-10}$	$3.5\,10^{-10}$	$8\,10^{-10}$
Pressure on particle P [Pa]	$4\,10^{1796}$	$1.7\,10^{1790}$	$1.6\,10^{1773}$	$3.6\,10^{1771}$	$1.6\,10^{1763}$	$1.6\,10^{1761}$	$5.5\,10^{1759}$	$1.6\,10^{1758}$	$3\,10^{491}$	10^{492}	$3.3\,10^{492}$	$1.2\,10^{493}$	$2\,10^{493}$	$3\,10^{258}$
Energy [J] **Total E**	$-1.8\,10^{49}$	$-2.3\,10^{43}$	$-7.5\,10^{25}$	$-1.6\,10^{24}$	$-7.5\,10^{15}$	$-7.5\,10^{13}$	$-2.3\,10^{12}$	$-7.5\,10^{10}$	$7.8\,10^{10}$	$1.2\,10^{12}$	$1.4\,10^{12}$	$1.7\,10^{12}$	$1.9\,10^{12}$	$1.9\,10^{12}$
Energy [J] U	$-1.8\,10^{49}$	$-2.3\,10^{43}$	$-7.5\,10^{25}$	$-1.6\,10^{24}$	$-7.5\,10^{15}$	$-7.5\,10^{13}$	$-2.3\,10^{12}$	$-7.5\,10^{10}$	$-7.7\,10^{9}$	-10^{9}	$-5.6\,10^{8}$	$-2.5\,10^{8}$	$-1.9\,10^{8}$	**$-2\,10^{8}$**
Energy [J] K	~ 0	10^{-94}	$4.3\,10^{-42}$	$4.4\,10^{-37}$	$4.3\,10^{-12}$	$4.3\,10^{-6}$	0.13	$4.3\,10^{3}$	$4.4\,10^{6}$	$6\,10^{7}$	$7\,10^{7}$	$9\,10^{7}$	10^{8}	**$2\,10^{8}$**
Energy [J] E_{rad}	$6\,10^{-108}$	$2.6\,10^{-90}$	$8.5\,10^{-38}$	$8.7\,10^{-33}$	$8.4\,10^{-8}$	$8.4\,10^{-2}$	$2.6\,10^{3}$	$8.4\,10^{7}$	$8.6\,10^{10}$	$1.2\,10^{12}$	$1.4\,10^{12}$	$1.7\,10^{12}$	$1.9\,10^{12}$	$1.9\,10^{12}$
T [°K] **@ SR** (from E_{rad})	10^{-29}	$2.5\,10^{-24}$	$3.4\,10^{-11}$	**$6.1\,10^{-10}$** ***Hawking***	10^{-3}	$3.4\,10^{-2}$	0.45	6	34	66	69	73	74	74
λ [m] **@ SR**	$3\,10^{25}$	10^{21}	$8.5\,10^{7}$	$4.7\,10^{6}$	2.7	$85\,10^{-3}$	$6.4\,10^{-3}$	$0.5\,10^{-3}$	$84\,10^{-6}$	$44\,10^{-6}$	$42\,10^{-6}$	$40\,10^{-6}$	$39\,10^{-6}$	$39\,10^{-6}$
Spectrum	*Undefined*		*ELF to VHF*			*Microwave to IR (FIR)*			*IR (FIR)*					
T [°K] **@ r** (from E_{rad})	$1.3\,10^{12}$	$4.4\,10^{10}$	$1.6\,10^{6}$	$4\,10^{4}$	$5.8\,10^{3}$	$1.8\,10^{3}$	$7.8\,10^{2}$	$3.3\,10^{2}$	$1.8\,10^{2}$	114	97	79	74.4	74
λ [m] **@ r**	$2\,10^{-15}$	$6.6\,10^{-14}$	$1.5\,10^{-9}$	$7\,10^{-8}$	$5\,10^{-7}$	$1.5\,10^{-6}$	$3.7\,10^{-6}$	$8.8\,10^{-6}$	$15\,10^{-6}$	$25\,10^{-6}$	$30\,10^{-6}$	$37\,10^{-6}$	$39\,10^{-6}$	$39\,10^{-6}$
Spectrum	γ		*X-rays*	*UV to Visible*		*IR*								

Figure 15

Radiation and particle data for a 100 solar mass black hole

$10^4\,M_\odot$ (Nucleus radius $3\,10^5$ [m])														
Particles' charge [C]	$q=\pm\frac{e}{3}$								$q=\pm\frac{2e}{3}$					$q=\pm e$
BH inner radius r [m]	$1.76\,10^{-77}$	10^{-61}	$4.8\,10^{-26}$	$5\,10^{-14}$	10^{-6}	10^{-2}	10	10^{4}	10^{6}	10^{7}	$1.5\,10^{7}$	$2.5\,10^{7}$	$2.95\,10^{7}$	**(SR)** $2.966\,10^{7}$
Particle radius r_0 [m]	$1.76\,10^{-77}$	$1.3\,10^{-69}$	$9.2\,10^{-52}$	$9.4\,10^{-46}$	$4.2\,10^{-42}$	$4.2\,10^{-40}$	$1.3\,10^{-38}$	$4.2\,10^{-37}$	$4.3\,10^{-36}$	$6.4\,10^{-36}$	$5\,10^{-36}$	$3.7\,10^{-36}$	$3.4\,10^{-36}$	$3.4\,10^{-36}$
Particle mass m [Kg]	$1.6\,10^{31}$	$2.2\,10^{23}$	$3\,10^{5}$	0.3	$7\,10^{-5}$	$7\,10^{-7}$	$2.2\,10^{-8}$	$7\,10^{-10}$	$3\,10^{-10}$	$1.8\,10^{-10}$	$2.3\,10^{-10}$	$3\,10^{-10}$	$3.3\,10^{-10}$	$7.5\,10^{-10}$
Pressure on particle P [Pa]	$4\,10^{1796}$	$5.5\,10^{1788}$	$7\,10^{1770}$	$7\,10^{1764}$	$1.6\,10^{1761}$	$1.6\,10^{1759}$	$5.5\,10^{1757}$	$1.6\,10^{1756}$	$3.3\,10^{489}$	$9\,10^{489}$	$3\,10^{490}$	10^{491}	$1.7\,10^{491}$	$2.5\,10^{256}$
Energy [J] **Total E**	$-1.8\,10^{51}$	$-2.3\,10^{43}$	$-3.4\,10^{25}$	$-3.4\,10^{19}$	$-7.5\,10^{15}$	$-7.5\,10^{13}$	$-2.3\,10^{12}$	$-7.5\,10^{10}$	$7.8\,10^{10}$	$1.3\,10^{12}$	$1.5\,10^{12}$	$1.8\,10^{12}$	$2\,10^{12}$	$2\,10^{12}$
Energy [J] U	$-1.8\,10^{51}$	$-2.3\,10^{43}$	$-3.4\,10^{25}$	$-3.4\,10^{19}$	$-7.5\,10^{15}$	$-7.5\,10^{13}$	$-2.3\,10^{12}$	$-7.5\,10^{10}$	$-7.7\,10^{9}$	-10^{9}	$-6\,10^{8}$	$-2.7\,10^{8}$	$-2\,10^{8}$	**$-2\,10^{8}$**
Energy [J] K	~ 0	$1.3\,10^{-94}$	$4.5\,10^{-41}$	$4.8\,10^{-23}$	$4\,10^{-12}$	$4\,10^{-6}$	0.13	$4.3\,10^{3}$	$4.4\,10^{6}$	$6.5\,10^{7}$	$7.7\,10^{7}$	$9.5\,10^{7}$	10^{8}	**$2\,10^{8}$**
Energy [J] E_{rad}	$6\,10^{-114}$	$2.6\,10^{-90}$	$8.9\,10^{-37}$	$9.5\,10^{-19}$	$8.4\,10^{-8}$	$8.4\,10^{-2}$	$2.6\,10^{3}$	$8.4\,10^{7}$	$8.6\,10^{10}$	$1.3\,10^{12}$	$1.5\,10^{12}$	$1.8\,10^{12}$	$2\,10^{12}$	$2\,10^{12}$
T [°K] **@ SR** (from E_{rad})	$3\,10^{-31}$	$2.5\,10^{-25}$	**$6.1\,10^{-12}$** ***Hawking***	$2\,10^{-7}$	10^{-4}	$3\,10^{-3}$	$4.5\,10^{-2}$	0.6	3.4	6.7	7	7.4	7.5	7.5
λ [m] **@ SR**	$9\,10^{27}$	10^{22}	$4.7\,10^{8}$	$1.5\,10^{4}$	27	0.85	$64\,10^{-3}$	$4.8\,10^{-3}$	$0.85\,10^{-3}$	$0.43\,10^{-3}$	$0.4\,10^{-3}$	$0.39\,10^{-3}$	$0.38\,10^{-3}$	$0.38\,10^{-3}$
Spectrum	*Undefined*		*Radio (from ELF to UHF)*			*Microwave*				*IR (FIR)*				
T [°K] **@ r** (from E_{rad})	$4\,10^{11}$	$4.4\,10^{9}$	$1.5\,10^{5}$	$4.8\,10^{3}$	$6\,10^{2}$	$1.85\,10^{2}$	78	33	18.6	11.6	9.8	7.9	7.5	7.5
λ [m] **@ r**	$7\,10^{-15}$	$6.6\,10^{-13}$	$1.9\,10^{-8}$	$6\,10^{-7}$	$5\,10^{-6}$	$16\,10^{-6}$	$37\,10^{-6}$	$88\,10^{-6}$	$155\,10^{-6}$	$0.25\,10^{-3}$	$0.29\,10^{-3}$	$0.36\,10^{-3}$	$0.38\,10^{-3}$	$0.38\,10^{-3}$
Spectrum	γ		*From EUV to FIR*											

Figure 16

Radiation and particle data for a 10,000 solar mass black hole

10^6 $M_\odot$ (Nucleus radius $3.3\ 10^7$ [m])														
Particles' charge [C]	$q=\pm\frac{e}{3}$								$q=\pm\frac{2e}{3}$					$q=\pm e$
BH inner radius r [m]	$1.76\ 10^{-79}$	10^{-59}	$1.5\ 10^{-26}$	$2\ 10^{-17}$	10^{-4}	1	10^3	10^6	10^8	10^9	$1.5\ 10^9$	$2.5\ 10^9$	$2.95\ 10^9$	(SR) $2.966\ 10^9$
Particle radius r_0 [m]	$1.76\ 10^{-79}$	$1.3\ 10^{-69}$	$4.2\ 10^{-53}$	$1.8\ 10^{-48}$	$4.2\ 10^{-42}$	$4.2\ 10^{-40}$	$1.3\ 10^{-38}$	$4.2\ 10^{-37}$	$4.3\ 10^{-36}$	$6.8\ 10^{-36}$	$5\ 10^{-36}$	$4\ 10^{-36}$	$3.6\ 10^{-36}$	$3.6\ 10^{-36}$
Particle mass m [Kg]	$1.6\ 10^{33}$	$2\ 10^{23}$	$6.8\ 10^6$	$1.6\ 10^2$	$7\ 10^{-5}$	$7\ 10^{-7}$	$2.2\ 10^{-8}$	$7\ 10^{-10}$	$2.6\ 10^{-11}$	$2\ 10^{-10}$	$2.3\ 10^{-10}$	$2.8\ 10^{-10}$	$3\ 10^{-10}$	$7\ 10^{-10}$
Pressure on particle P [Pa]	$4\ 10^{1796}$	$5\ 10^{1786}$	$2\ 10^{1770}$	$4\ 10^{1765}$	$1.6\ 10^{1759}$	$1.6\ 10^{1757}$	$5.5\ 10^{1755}$	$1.6\ 10^{1754}$	$3\ 10^{486}$	$9\ 10^{487}$	$3\ 10^{488}$	$9\ 10^{488}$	$1.4\ 10^{489}$	$2\ 10^{254}$
Energy [J] **Total E**	$-1.8\ 10^{53}$	$-2.3\ 10^{43}$	$-7.5\ 10^{26}$	$-1.6\ 10^{22}$	$-7.5\ 10^{15}$	$-7.5\ 10^{13}$	$-2.3\ 10^{12}$	$-7.5\ 10^{10}$	$7.8\ 10^{10}$	$1.36\ 10^{12}$	$1.5\ 10^{12}$	$2\ 10^{12}$	$2\ 10^{12}$	$2\ 10^{12}$
U	$-1.8\ 10^{53}$	$-2.3\ 10^{43}$	$-7.5\ 10^{26}$	$-1.6\ 10^{22}$	$-7.5\ 10^{15}$	$-7.5\ 10^{13}$	$-2.3\ 10^{12}$	$-7.5\ 10^{10}$	$-7.8\ 10^9$	$-1.2\ 10^9$	$-6\ 10^8$	$-2.9\ 10^8$	$-2.2\ 10^8$	$-2\ 10^8$
K	~ 0	$1.3\ 10^{-94}$	$4.3\ 10^{-43}$	$3.7\ 10^{-31}$	$4.3\ 10^{-12}$	$4.3\ 10^{-6}$	$1.3\ 10^{-1}$	$4.3\ 10^3$	$4.4\ 10^6$	$7\ 10^7$	$8\ 10^7$	10^8	$1.1\ 10^8$	$2\ 10^8$
E_{rad}	$6.3\ 10^{-120}$	$2.6\ 10^{-90}$	$8.5\ 10^{-41}$	$7\ 10^{-27}$	$8.4\ 10^{-8}$	$8.4\ 10^{-2}$	$2.6\ 10^3$	$8.4\ 10^7$	$8.6\ 10^{10}$	$1.36\ 10^{12}$	$1.5\ 10^{12}$	$2\ 10^{12}$	$2\ 10^{12}$	$2\ 10^{12}$
T [°K] @ SR (from E_{rad})	10^{-33}	$2.5\ 10^{-26}$	$6.1\ 10^{-14}$ *Hawking*	$1.8\ 10^{-10}$	10^{-5}	$3.4\ 10^{-4}$	$4.5\ 10^{-3}$	$6\ 10^{-2}$	0.3	0.7	0.7	0.75	0.76	0.76
λ [m] @ SR	$2.9\ 10^{30}$	10^{23}	$4.7\ 10^{10}$	$1.6\ 10^7$	$2.7\ 10^2$	8.5	0.6	$48\ 10^{-3}$	$8.5\ 10^{-3}$	$4\ 10^{-3}$	$4\ 10^{-3}$	$3.9\ 10^{-3}$	$3.8\ 10^{-3}$	$3.8\ 10^{-3}$
Spectrum	*Undefined*		*Radio (from < ELF to VHF)*				*Microwave*							
T [°K] @ r (from E_{rad})	$1.3\ 10^{11}$	$4.4\ 10^8$	$3\ 10^4$	$2.2\ 10^3$	58.7	18.5	7.8	3.3	1.8	1.2	0.98	0.82	0.76	0.76
λ [m] @ r	$2.2\ 10^{-14}$	$6.6\ 10^{-12}$	$8.8\ 10^{-8}$	$1.3\ 10^{-6}$	$49\ 10^{-6}$	$156\ 10^{-6}$	$0.37\ 10^{-3}$	$0.88\ 10^{-3}$	$1.5\ 10^{-3}$	$2.5\ 10^{-3}$	$2.9\ 10^{-3}$	$3.5\ 10^{-3}$	$3.8\ 10^{-3}$	$3.8\ 10^{-3}$
Spectrum	γ		*From EUV to IR*					*Microwave*						

Figure 17

Radiation and particle data for a 1 million solar mass black hole

10^{11} $M_\odot$ (Nucleus radius $4.5\ 10^{12}$ [m])														
Particles' charge [C]	$q=\pm\frac{e}{3}$								$q=\pm\frac{2e}{3}$					$q=\pm e$
BH inner radius r [m]	$1.76\ 10^{-84}$	10^{-54}	$2.2\ 10^{-28}$	$2\ 10^{-12}$	10	10^5	10^8	10^{11}	10^{13}	10^{14}	$1.5\ 10^{14}$	$2.5\ 10^{14}$	$2.95\ 10^{14}$	(SR) $2.966\ 10^{14}$
Particle radius r_0 [m]	$1.76\ 10^{-84}$	$1.3\ 10^{-69}$	$2\ 10^{-56}$	$2\ 10^{-48}$	$4.2\ 10^{-42}$	$4.2\ 10^{-40}$	$1.3\ 10^{-38}$	$4.2\ 10^{-37}$	$4.3\ 10^{-36}$	$8.4\ 10^{-36}$	$6\ 10^{-36}$	$4.7\ 10^{-36}$	$4.3\ 10^{-36}$	$4.2\ 10^{-36}$
Particle mass m [Kg]	$1.6\ 10^{38}$	$2.2\ 10^{23}$	$1.4\ 10^{10}$	$1.5\ 10^2$	$7\ 10^{-5}$	$7\ 10^{-7}$	$2.2\ 10^{-8}$	$7\ 10^{-10}$	$3\ 10^{-10}$	$1.3\ 10^{-10}$	$2\ 10^{-10}$	$2.4\ 10^{-10}$	$2.7\ 10^{-10}$	$6\ 10^{-10}$
Pressure on particle P [Pa]	$4\ 10^{1796}$	$5.5\ 10^{1781}$	$3\ 10^{1768}$	$3\ 10^{1760}$	$1.6\ 10^{1754}$	$1.6\ 10^{1752}$	$5.5\ 10^{1750}$	$1.6\ 10^{1749}$	$3\ 10^{482}$	$4\ 10^{482}$	$2\ 10^{483}$	$5.5\ 10^{483}$	$9\ 10^{483}$	10^{249}
Energy [J] **Total E**	$-1.8\ 10^{58}$	$-2.3\ 10^{43}$	$-1.6\ 10^{30}$	$-1.7\ 10^{22}$	$-7.5\ 10^{15}$	$-7.5\ 10^{13}$	$-2.3\ 10^{12}$	$-7.5\ 10^{10}$	$7.8\ 10^{10}$	$1.7\ 10^{12}$	$1.9\ 10^{12}$	$2.3\ 10^{12}$	$2.5\ 10^{12}$	$2.5\ 10^{12}$
U	$-1.8\ 10^{58}$	$-2.3\ 10^{43}$	$-1.6\ 10^{30}$	$-1.7\ 10^{22}$	$-7.5\ 10^{15}$	$-7.5\ 10^{13}$	$-2.3\ 10^{12}$	$-7.5\ 10^{10}$	$-7.7\ 10^9$	$-1.5\ 10^9$	$-7.5\ 10^8$	$-3.4\ 10^8$	$-2.6\ 10^8$	$-2.6\ 10^8$
K	0	$1.3\ 10^{-94}$	$4.4\ 10^{-55}$	$4\ 10^{-31}$	$4.3\ 10^{-12}$	$4.3\ 10^{-6}$	0.13	$4.3\ 10^3$	$4.4\ 10^6$	$8.6\ 10^7$	$9.7\ 10^7$	$1.2\ 10^8$	$1.3\ 10^8$	$2.6\ 10^8$
E_{rad}	$6.3\ 10^{-135}$	$2.6\ 10^{-90}$	$9\ 10^{-51}$	$7.5\ 10^{-27}$	$8.4\ 10^{-8}$	$8.4\ 10^{-2}$	$2.6\ 10^3$	$8.4\ 10^7$	$8.6\ 10^{10}$	$1.7\ 10^{12}$	$1.9\ 10^{12}$	$2.3\ 10^{12}$	$2.5\ 10^{12}$	$2.5\ 10^{12}$
T [°K] @ SR (from E_{rad})	$5.6\ 10^{-40}$	$8\ 10^{-29}$	$6.1\ 10^{-19}$ *Hawking*	$5.9\ 10^{-13}$	$3.4\ 10^{-8}$	10^{-6}	$1.4\ 10^{-5}$	$1.9\ 10^{-4}$	10^{-3}	$2.3\ 10^{-3}$	$2.3\ 10^{-3}$	$2.5\ 10^{-3}$	$2.5\ 10^{-3}$	$2.5\ 10^{-3}$
λ [m] @ SR	$5\ 10^{36}$	$4\ 10^{25}$	$4.7\ 10^{15}$	$5\ 10^9$	$8.5\ 10^4$	$2.7\ 10^3$	$2\ 10^2$	15	2.7	1.3	1.24	1.17	1.15	1.15
Spectrum	*Undefined*			*Radio (from < ELF to VHF)*										
T [°K] @ r (from E_{rad})	$7\ 10^9$	$1.4\ 10^6$	$7\ 10^2$	7.2	0.18	$6\ 10^{-2}$	$2.4\ 10^{-2}$	10^{-2}	$6\ 10^{-3}$	$4\ 10^{-3}$	$3.3\ 10^{-3}$	$2.7\ 10^{-3}$	$2.5\ 10^{-3}$	$2.5\ 10^{-3}$
λ [m] @ r	$4\ 10^{-13}$	$2\ 10^{-9}$	$4\ 10^{-6}$	$0.4\ 10^{-3}$	$16\ 10^{-3}$	$49\ 10^{-3}$	$118\ 10^{-3}$	$278\ 10^{-3}$	$492\ 10^{-3}$	$740\ 10^{-3}$	0.88	1	1.15	1.15
Spectrum	γ	*X-rays*	*IR*	*Microwave*										

Figure 18

Radiation and particle data for a 100 thousand million solar mass black hole

Gravitational Redshift Derived from the Universal Electrodynamic Total Energy Equation

The universal total energy Eq. (16) is the first and only one in physics accounting not only for velocity but also for acceleration as another kinetic variable in the dynamic of the system. It is a true total energy equation with such an extent that it can explain the behavior of Mother Nature as no other theory can.

Currently there are some discrepancies in the measurements of cosmological distances, such as the so-called "Hubble tension." These discrepancies may be due to several factors.

Possible Factors of Discrepancy in Cosmological Distance Measurements

1. Mother Nature tells us through the more than proven laws of electrodynamics that **the universe must have a center**. Just because we haven't discovered it yet doesn't mean it doesn't exist. The theoretical proof is that the universal force laws depend on $\frac{1}{r^2}$.

2. Masses in the universe may be organized around a "master black hole" at the center of the universe by following the quantized orbits law of the new gravitational force (approximated by the Titius-Bode law).

3. Orbiting masses around the central "master black hole" will be subject to an increase or decrease of their relative velocity. This fact doesn't strictly mean that masses are "receding" because the universe is expanding. The theory of "universe expansion" will become invalid if the universe has a center.

4. As proved in the study Astronomical Distance Measurements Are Wrong [17], **EMWs from a rotating source do not follow an astronomical straight line but an Archimedes spiral path**. This fact indicates that all measurements we make by using the cosmic ladder technique are wrong. Thus, real distances must all be shorter than we now know.

5. Redshift is usually calculated from formulas derived from the invalid, obsolete, and ill-fated theory of relativity that completely dismiss acceleration and the variables of the type of motion. Next, we'll find the gravitational redshift from the universal total energy equation, which will show that the angle between the acceleration direction of the source with respect to the measurement line will greatly influence the calculation. Matching measurements with calculations may tell us in which direction the source is accelerating. **In all cases and according to point 4, more real distance calculations have to be made in order to determine more real redshifts.**

Derivation of the Gravitational Redshift from the Universal Total Energy Equation

As we already know, gravity is an EMW that can give us information about the decrease of the lump Newtonian mass of the cosmic object because of radiation loss. Therefore, the gravitational potential energy on the surface area of a radiating cosmic object is intimately linked to this process.

Derivation of the Gravitational Redshift from the Schwarzschild Radius

The maximum change in potential energy occurs between zero energy at a theoretically infinite distance and the maximum energy, which is given by the Schwarzschild radius Eq. (21) that we recall here.

$r_s = -\frac{2\cos(\alpha)GM}{c^2\left(1-\frac{v^2}{c^2}\right)}$ (59)

Dividing both sides of Eq. (59) by the real radius, we get a dimensionless expression with the radii ratio on the left-hand side and a potential energy related right-hand side:

$\frac{r_s}{r} = -\frac{2\cos(\alpha)GM}{r\,c^2\left(1-\frac{v^2}{c^2}\right)}$ (60)

This ratio is defined as the fractional change in wavelength, or redshift, relating the wavelength at infinity with the wavelength at the surface area given by the radius *r*.

$z = \frac{\Delta\lambda}{\lambda} = \frac{\lambda_\infty - \lambda}{\lambda} = \frac{\lambda_\infty}{\lambda} - 1$, or $z + 1 = \frac{\lambda_\infty}{\lambda}$ (61). Thus, we can write Eq. (60) as follows:

$\frac{\lambda_\infty}{\lambda} = -\frac{2\cos(\alpha)GM}{rc^2\left(1-\frac{v^2}{c^2}\right)}$ (62)

Where α is the angle between $\vec{r}$ and $\vec{a}$. Note that for this quantity to be positive, the angle must be $\frac{\pi}{2} < \alpha < \frac{3\pi}{2}$. Observe that the relative velocity is already taken into account in the same equation so that no Doppler correction is needed.

It is also important to note that the equations derived in the theory of relativity lack the angular variable, so they are only valid in the very special case when $\alpha = \frac{2\pi}{3}$ and $v << c$, which makes Eq. (62) as follows:

$\frac{\lambda_\infty}{\lambda} = \frac{G\,M}{rc^2}$ (63)

In general, for the angle range $\frac{\pi}{2} < \alpha < \frac{3\pi}{2}$, our redshift equation becomes:

$\frac{\lambda_\infty}{\lambda} = \frac{2\cos(\alpha)GM}{rc^2\left(1-\frac{v^2}{c^2}\right)}$ (64)

Where the factor $2\cos(\alpha)$ will greatly influence the result of the calculation.

Derivation of the Gravitational Redshift from the Wavelength Equation

We can obtain the wavelength of a radiation by equating the universal total energy Eq. (16) with the Planck equation:

$$\frac{h\,c}{\lambda} = \gamma_E\left(kq_1q_2\left(\frac{1}{r_f} - \frac{1}{r_i}\right) - \frac{kq_1q_2}{c^2}\left(\frac{1}{r_f} - \frac{1}{r_i}\right)v^2 + \frac{2kq_1q_2\,cos(\alpha)}{c^2}\left(ln(r_i) - ln(r_f)\right)a\right)$$

$$\lambda = \frac{h\,c^3 r_f r_i}{\gamma_E kq_1q_2\left(2\cos(\alpha)ar_f r_i(\ln(r_i) - \ln(r_f)) + c^2\left(1-\frac{v^2}{c^2}\right)(r_i - r_f)\right)} \quad (65)$$

Assuming that at a large distance $r_f = r_1$ we have a wavelength λ_1, and λ_2 at a distance $r_f = r_2$:

$$\lambda_1 = \frac{h\,c^3 r_1 r_i}{\gamma_E kq_1q_2\left(2\cos(\alpha)ar_1 r_i(\ln(r_i) - \ln(r_1)) + c^2\left(1-\frac{v^2}{c^2}\right)(r_i - r_1)\right)}$$

$$\lambda_2 = \frac{h\, c^3 r_2 r_i}{\gamma_E k q_1 q_2 \left(2\cos(\alpha) a r_2 r_i (\ln(r_i) - \ln(r_2)) + c^2 \left(1 - \frac{v^2}{c^2}\right)(r_i - r_2)\right)}$$

The redshift is defined as the fractional change in wavelength: $z = \frac{\Delta\lambda}{\lambda} = \frac{\lambda_2 - \lambda_1}{\lambda_1} = \frac{\lambda_2}{\lambda_1} - 1$, or $z + 1 = \frac{\lambda_2}{\lambda_1}$.

If the acceleration is caused by a gravitational force, we can replace it by $a = \frac{GM}{r_2^2}$. Thus, the gravitational redshift of the object with mass M and radius r_2 is:

$$z + 1 = \frac{\lambda_2}{\lambda_1} = \left| \frac{\frac{1}{2}\left(-2GMr_1 r_i (\ln(r_i) - \ln(r_1))\cos(\alpha) + r_2^2 c^2 \left(1 - \frac{v^2}{c^2}\right)(r_1 - r_i)\right)}{\left(GMr_i(\ln(r_2) - \ln(r_i))\cos(\alpha) + \frac{1}{2} r_2 c^2 \left(1 - \frac{v^2}{c^2}\right)(r_2 - r_i)\right) r_1} \right| \quad (66)$$

Taking the initial distance as $r_i = 10^{27}[m]$ usually is good enough to replace the irreal "infinity" value. The farthest distance and the angle will greatly influence the result of the calculation. Very good results are obtained when choosing $r_1 = 0.6\, r_i$ (that gives approximately the oldest observed light) and an angle between $\frac{2\pi}{3} \le \alpha \le \pi$.

Important Word of Caution About Redshift

Astronomers and astrophysicists should exercise extreme precautions when measuring and calculating redshifts.

Conflicts in distances may arise due to the causes detailed in previous paragraphs and specifically because light from rotating sources does not follow a straight line but an Archimedean spiral path, so all distance measurements are larger than they should be.

Our universe works based on physics laws that are valid on any scale, like the universal laws of electrodynamics. Invented, unphysical, and unsubstantiated theories will only hinder and destroy the pursuit of real-world knowledge.

Particle Orbits Around a Black Hole and the Origin of "Astrophysical Jets"

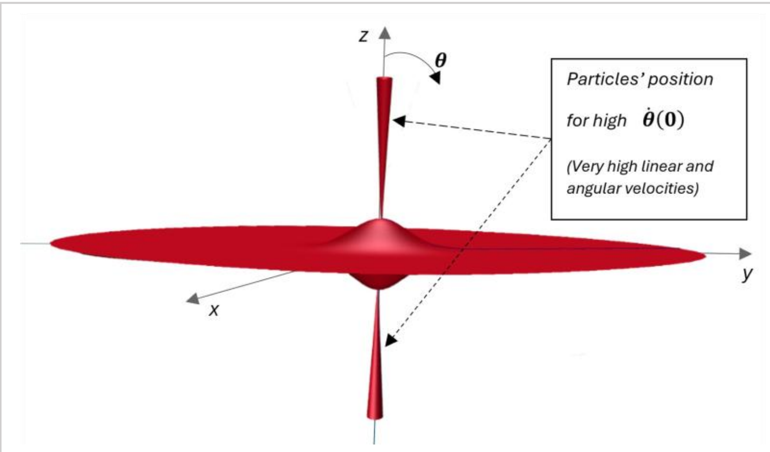

Figure 19

Position of masses around a central mass according to gravitational law. It is also valid for black holes.

In the study Full Free Motion of Celestial Bodies Around a Central Mass – Why Do They Mostly Orbit in the Equatorial Plane? [18], the position of an orbiting mass around a much bigger central mass was examined in detail. Though the differential equations of motion were derived based on Newton's basic gravitational law, the results showed that from a certain distance onwards, masses reach equilibrium on the equatorial plane, i.e., for $\theta = \frac{\pi}{2}$, as shown in Fig. 19.

A different scenario happens at shorter distances, where masses may find equilibrium at any position around the central mass.

It was also shown that masses can reach equilibrium positions along the rotational axis of the central mass, depending on their initial angular velocity.

Later we will see that **the solution of the differential equations of motion of the new gravitational law will add important new details about the orbit of masses around a central mass**, which are absent when applying Newton's gravitational law.

Do Non-Rotating Black Holes Exist?

The answer is a resounding no.

A hypothetical non-rotating central mass can never hold the masses around, causing chaos in the universe. There will be no equilibrium and a violation of energy conservation.

Particle Motion Around a Black Hole

The analysis of particle motion from the new gravitational law will be made by solving the system of differential equations (13), (14), and (15). The differential equations will be solved for $1M_{\odot}$ black hole. For other BHs there will only be a change in the scale of the parameters and initial conditions, but no difference in the type of motions.

Even when results are somewhat similar to those obtained with Newton's gravitational law, new characteristics and properties in the motion will be made evident.

Looking at Fig. 3, our black hole will be located at the origin of coordinates and identified with mass m_1 and radius R_1, while the particle, being a proton or electron, is identified with mass m_2 and radius R_2. There is no difference in motion between the two particles.

Angular Momentum and Angular Velocity of a Black Hole

To solve the system of differential equations, one of the data we need is the angular velocity of the BH. Assuming that the BH is spherical, the angular momentum is $L = \frac{2}{5}MR^2\omega$. Replacing the radius by the SR ($R = \frac{2GM}{c^2}$), we get the angular momentum of the black hole:

$$L_{bh} = \frac{8}{5}\frac{M^3G^2\omega_{bh}}{c^4} \quad (67)$$

Assume that the star radius before becoming a BH is R_s and after becoming a BH is R_{bh}. If the mass keeps constant, since angular momentum is conserved, we have $L_s = L_{bh}$:

$\frac{2}{5}MR_s^2\omega_s = \frac{2}{5}MR_{bh}^2\omega_{bh}$, that is $\omega_{bh} = \frac{R_s^2\omega_s}{R_{bh}^2}$ (68). Replacing the radius of the BH $R_{bh} = \frac{2GM}{c^2}$ in Eq. (68) will give us the following expression for the angular velocity of a black hole:

$$\omega_{bh} = \frac{R_s^2c^4\omega_s}{4G^2M^2} \quad (69)$$

As our example BH is of $1M_{\odot}$, we'll take the angular velocity of the sun at mid-latitudes to be $\omega_s = 2.67\ 10^{-6}[\frac{rad}{s}]$ and an average sun radius at its equator of $R_s = 6.957\ 10^8[m]$, that will give a BH angular velocity of:

$$\omega_{bh} = 1.47\ 10^5\ [\frac{rad}{s}]$$

(Note that the "relativistic" formula $\omega_{bh} = \frac{c^3}{2GM}$ will give a lower value of $\omega_{bh} = 1.01\ 10^5[\frac{rad}{s}]$).

With this information we'll solve the system of differential equations for diverse initial conditions as an example and show how a particle like an electron or proton behaves under such conditions. Note that polar graphs are rotated in order to match the zero-axis with the polar angle in spherical coordinates. Results for diverse initial conditions are shown in Figs. (20), (21), (22), (23), and (24).

$r(0) = 2.976\ 10^3\,[m]$ (10 m away from the SR), $\dot{r}(0) = 10^4 \left[\frac{m}{s}\right]$		$\dot{\theta}(0) = 0 \left[\frac{rad}{s}\right]$		$\phi(0) = 0\,[rad]$, $\dot{\phi}(0) = 0 \left[\frac{rad}{s}\right]$	
$\theta(0)\ [rad]$	$\frac{\pi}{10^4}$ $(\theta \approx 0°)$	$\frac{\pi}{4}$	$\frac{\pi}{2}$	$\frac{3\pi}{4}$	π
$r(t)\ [m]$	*Particle reaches the SR after $t \approx 4.3\ 10^{-9}\,[s]$ and is captured by the BH* 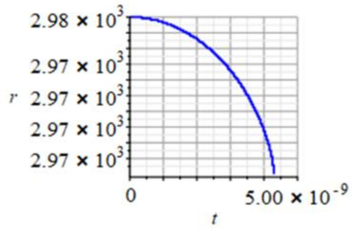	Same as for $\frac{\pi}{10^4}$	Same as for $\frac{\pi}{10^4}$	Same as for $\frac{\pi}{10^4}$	Same as for $\frac{\pi}{10^4}$
$\dot{r}(t) \left[\frac{m}{s}\right]$	*Relative velocity increases far beyond c when particle is captured at the SR* 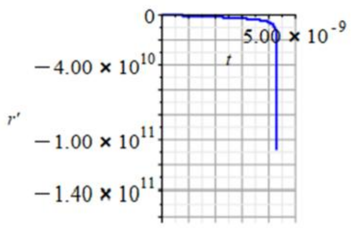	Same as for $\frac{\pi}{10^4}$	Same as for $\frac{\pi}{10^4}$	Same as for $\frac{\pi}{10^4}$	Same as for $\frac{\pi}{10^4}$
$\theta(t)\ [rad]$	$\theta \approx 0$	$\theta \approx \frac{\pi}{4}$	$\theta \approx \frac{\pi}{2}$	$\theta \approx \frac{3\pi}{4}$	$\theta \approx \pi$
$\dot{\theta}(t) \left[\frac{rad}{s}\right]$	$\dot{\theta} \approx 0$	$\dot{\theta} \approx 0$	$\dot{\theta} \approx 0$	$\dot{\theta} \approx 0$	$\dot{\theta} \approx 0$
$\phi(t)\ [rad]$	$\phi \approx 0$	$\phi \approx 0$	$\phi \approx 0$	$\phi \approx 0$	$\phi \approx 0$
$\dot{\phi}(t) \left[\frac{rad}{s}\right]$	$\dot{\phi} \approx 0$	$\dot{\phi} \approx 0$	$\dot{\phi} \approx 0$	$\dot{\phi} \approx 0$	$\dot{\phi} \approx 0$

Figure 20

Particle capture. The particle is captured by the black hole also for initial positions $r(0) = 6\ 10^3, 10^4, 60\ 10^3, 10^5 [m]$

In Fig. 20 we see how the BH captures the particle immediately. Most probably, the particle may fuse with another one at the Schwarzschild radius before reaching the interior of the black hole. The graph of velocity is for free particle motion inside the BH, something that will never happen in the real world.

By keeping the same angular initial conditions, the BH will also capture the particle for the following particle's initial positions: $\mathrm{r}(0) = 6\ 10^3, 10^4, 60\ 10^3, 10^5 [\mathrm{m}]$.

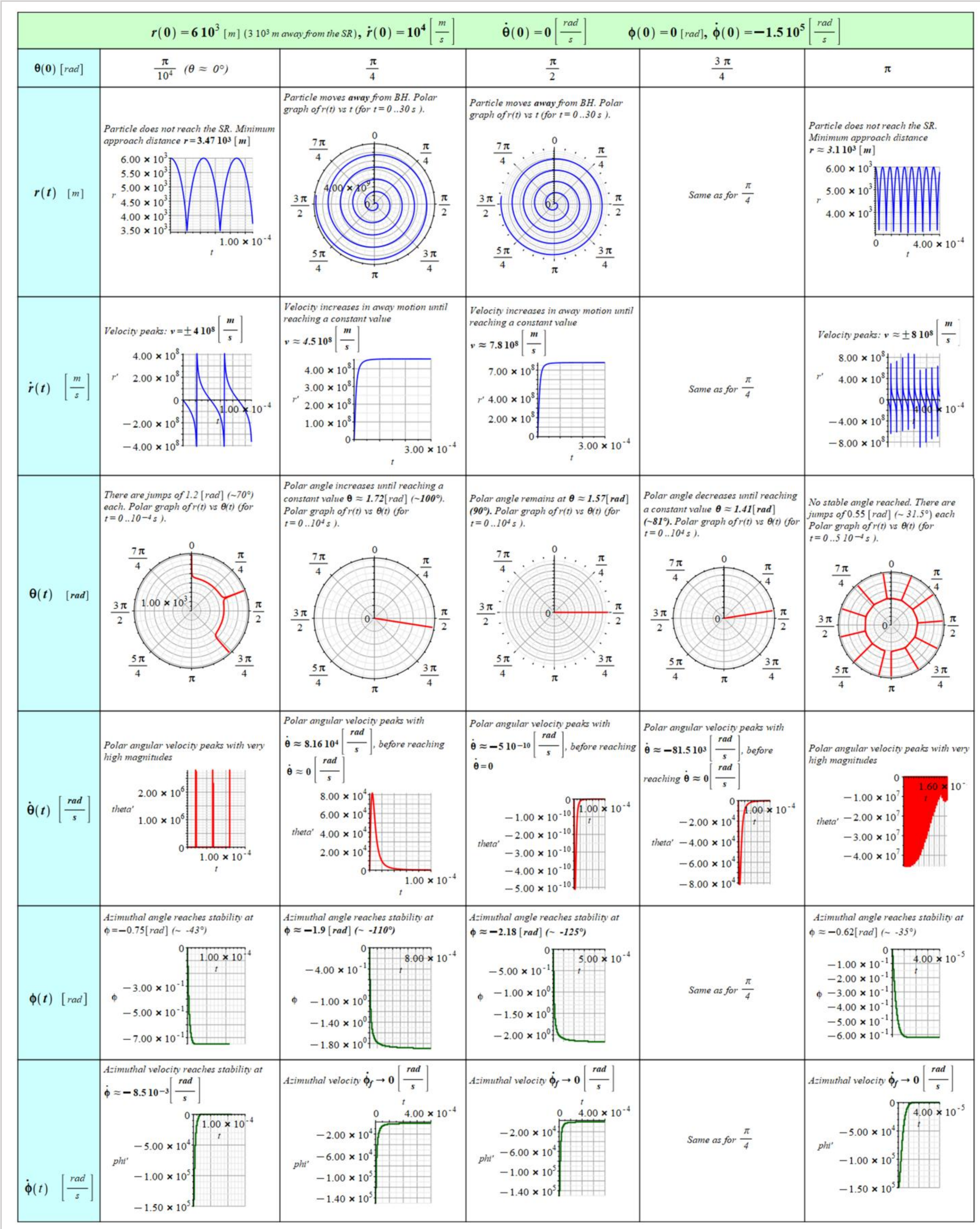

Figure 21

The particle is not captured by the black hole. The particle orbits the BH at a distance near its initial position and jumps away and back at discrete angular positions with extreme velocity.

Fig. 21 we see that the particle is not captured by the black hole. In the first and last columns of the table it is shown how the particle orbits the BH at a distance near its initial position and jumps away and back at discrete angular positions with extreme velocity.

By inspecting the remaining columns, it is clearly seen that the particle escapes from the BH at about its equatorial plane and reaches a constant velocity after some time.

$r(0)=6\,10^3$ [m] (3 10³ m away from the SR), $\dot{r}(0)=10\left[\frac{m}{s}\right]$ $\dot{\theta}(0)=10^{-7}\left[\frac{rad}{s}\right]$ $\phi(0)=0$ [rad], $\dot{\phi}(0)=10^{-5}\left[\frac{rad}{s}\right]$					
$\theta(0)$ [rad]	$\frac{\pi}{10^4}$ ($\theta \approx 0°$)	$\frac{\pi}{4}$	$\frac{\pi}{2}$	$\frac{3\pi}{4}$	π
$r(t)$ [m]	Oscillatory. Particle does not reach the SR. Minimum approach distance $r \approx 3.1\,10^3$ [m]	Same as for $\frac{\pi}{10^4}$	Same as for $\frac{\pi}{10^4}$	Same as for $\frac{\pi}{10^4}$	Same as for $\frac{\pi}{10^4}$
$\dot{r}(t)$ $\left[\frac{m}{s}\right]$	Oscillatory. Velocity peaks: $v = \pm 8.8\,10^8 \left[\frac{m}{s}\right]$	Same as for $\frac{\pi}{10^4}$	Same as for $\frac{\pi}{10^4}$	Same as for $\frac{\pi}{10^4}$	Same as for $\frac{\pi}{10^4}$
$\theta(t)$ [rad]	Polar angle increases, with jumps of ~0.6 [rad] (~ 35°) each. Polar graph of r(t) vs θ(t) (for $t = 0..4\,10^{-4}$ s). 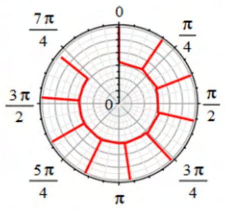	Polar angle increases, with jumps of ~0.6 [rad] (~ 35°) each. Polar graph of r(t) vs θ(t) (for $t = 0..10^{-3}$ s). 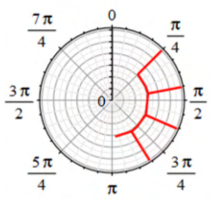	Polar angle increases, with jumps of ~0.6 [rad] (~ 35°) each. Polar graph of r(t) vs θ(t) (for $t = 0..10^{-4}$ s). 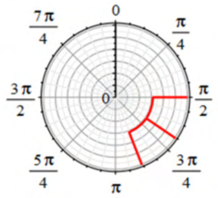	Polar angle increases, with jumps of ~0.6 [rad] (~ 35°) each. Polar graph of r(t) vs θ(t) (for $t = 0..7\,10^{-5}$ s). 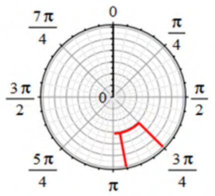	Polar angle decreases, with jumps of ~0.6 [rad] (~ 35°) each. Polar graph of r(t) vs θ(t) (for $t = 0..10^{-4}$ s). 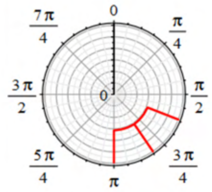
$\dot{\theta}(t)$ $\left[\frac{rad}{s}\right]$	Polar angular velocity peaks with very high magnitudes 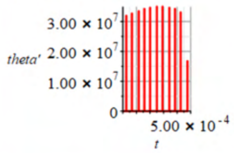	Similar to $\frac{\pi}{10^4}$	Similar to $\frac{\pi}{10^4}$	Similar to $\frac{\pi}{10^4}$	Polar angular velocity peaks with very high magnitudes 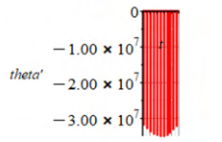
$\phi(t)$ [rad]	$\phi \approx 0$ [rad]	$\phi \approx 0$ [rad]	$\phi \approx 0$ [rad]	$\phi \approx 0$ [rad]	Azimuthal angle reaches stability at $\phi \approx 1.29$[rad] (~ 74°) 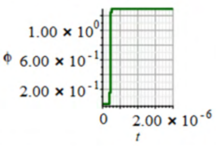
$\dot{\phi}(t)$ $\left[\frac{rad}{s}\right]$	$\dot{\phi} \approx 0 \left[\frac{rad}{s}\right]$	$\dot{\phi} \approx 0 \left[\frac{rad}{s}\right]$	$\dot{\phi} \approx 0 \left[\frac{rad}{s}\right]$	$\dot{\phi} \approx 0 \left[\frac{rad}{s}\right]$	After peaking at very high magnitude, the azimuthal velocity $\dot{\phi}_f \to 0 \left[\frac{rad}{s}\right]$ 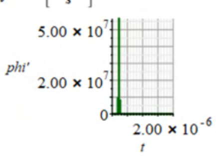

Figure 22

The particle is not captured by the black hole and does not escape either. The particle orbits the BH at a distance near its initial position and jumps away and back at discrete angular positions with extreme velocity.

In Fig. 22 we see that the particle is not captured by the black hole and does not escape either. The particle orbits the BH at a distance close to its original position, then jumps away and back with high velocity at angular positions, independent of the initial angular position.

$r(0)=60\ 10^3\ [m]$ (~57 10^3 m away from the SR), $\dot{r}(0)=10^2\left[\frac{m}{s}\right]$			$\dot{\theta}(0)=1.1\left[\frac{rad}{s}\right]$	$\phi(0)=0\ [rad]$, $\dot{\phi}(0)=10^3\left[\frac{rad}{s}\right]$	
$\theta(0)\ [rad]$	$\frac{\pi}{10^4}$ ($\theta \approx 0°$)	$\frac{\pi}{4}$	$\frac{\pi}{2}$	$\frac{3\pi}{4}$	π
$r(t)\ [m]$	*Oscillatory. Particle does not reach the SR. Minimum approach distance* $r=3.75\ 10^3\ [m]$	*Amplitude modulation. Particle moves from around its initial position up to* $r \approx 1.55\ 10^5 [m]$ ***away*** 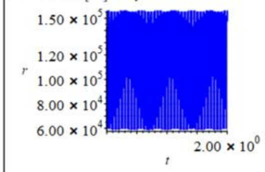	*Particle moves continuously away from its initial position and from the BH. Polar graph of r(t) vs t (for t = 0 ..30 s).* 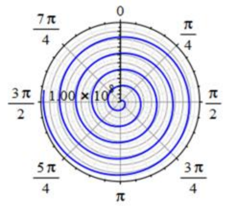	*Same as for* $\frac{\pi}{4}$	*Same as for* $\frac{\pi}{10^4}$
$\dot{r}(t)\ \left[\frac{m}{s}\right]$	*Oscillatory. Velocity peaks:* $v \approx \pm 3.5\ 10^8 \left[\frac{m}{s}\right]$ *Distance vs. velocity (for* $t=0..5\ 10^{-3}$ *s):* 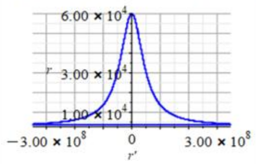	*Oscillatory. Velocity peaks:* $v \approx \pm 1.3\ 10^7\left[\frac{m}{s}\right]$ *Distance vs. velocity (for* $t=0..10^{-1}$ *s):* 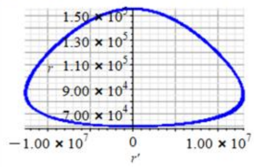	*Velocity peaks to* $v \approx 3.8\ 10^7\left[\frac{m}{s}\right]$ *before reaching a constant value* $v \approx 3.3\ 10^7\left[\frac{m}{s}\right]$ 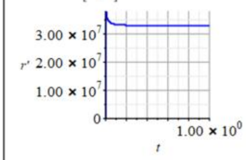	*Same as for* $\frac{\pi}{4}$	*Same as for* $\frac{\pi}{10^4}$
$\theta(t)\ [rad]$	*Few oscillations at 0,* $\frac{\pi}{2}$ *and* π. *Polar graph of r(t) vs θ(t) (for* $t=0..5\ 10^{-2}$ *s).* 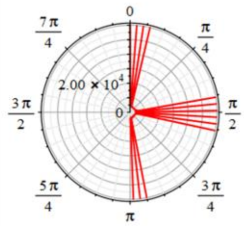	*Angle modulation, oscillating between* $\frac{\pi}{4}$ *and* $\frac{3\pi}{4}$. *Polar graph of r(t) vs θ(t) (for t = 0 ..0.3 s).* 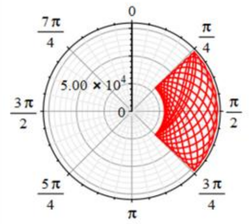	*Polar angle remains at* $\theta \approx \frac{\pi}{2}[rad]$. *Polar graph of r(t) vs θ(t) (for t = 0 ..30 s).* 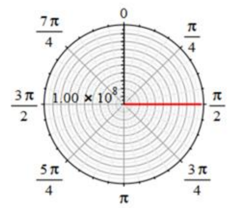	*Same as for* $\frac{\pi}{4}$	*Polar graph of r(t) vs θ(t) (for* $t=0..2.5\ 10^{-2}$ *s).* 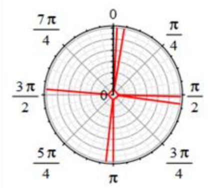
$\dot{\theta}(t)\ \left[\frac{rad}{s}\right]$	*Polar angular velocity peaks with very high magnitudes* 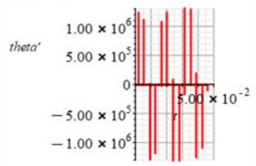	*Modulation of polar angular velocity, peaking to high magnitudes* 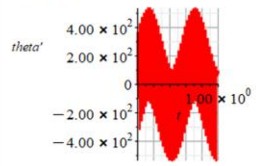	*Polar angular velocity reaches* $\dot{\theta} \approx 0$ *after a short time* 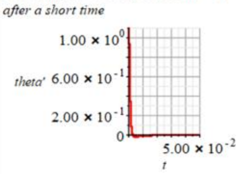	*Polar angular velocity peaks with high magnitudes* 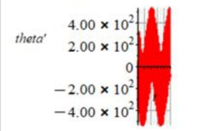	*Polar angular velocity peaks with very high magnitudes* 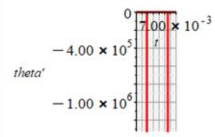
$\phi(t)\ [rad]$	*Azimuthal angle increases at discrete steps* 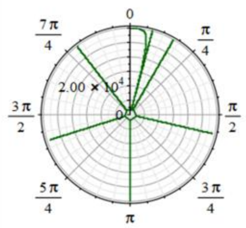	*The azimuthal angle of the particle's orbit around the BH shifts at discrete steps* 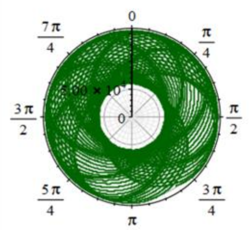	*Azimuthal angle reaches stability at* $\phi \approx 2.18\ [rad]$ *(~125°)* 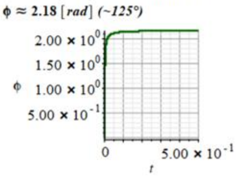	*Same as for* $\frac{\pi}{4}$	*Azimuthal angle reaches stability at* $\phi \approx 2.1[rad]$ *(~120°) with an extremely fast jump* 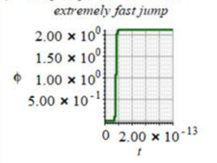
$\dot{\phi}(t)\ \left[\frac{rad}{s}\right]$	*Azimuthal velocity peaks to more than double its initial value.* 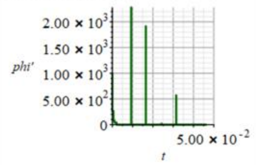	*Modulation of azimuthal velocity* 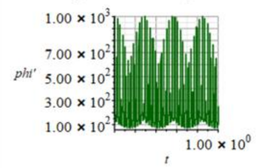	*Azimuthal velocity* $\dot{\phi}_f \to 0\left[\frac{rad}{s}\right]$ 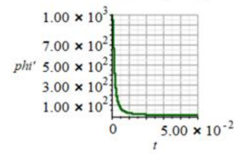	*Same as for* $\frac{\pi}{4}$	*Extremely fast and high magnitude of azimuthal velocity before reaching* $\dot{\phi}_f \to 0\left[\frac{rad}{s}\right]$ 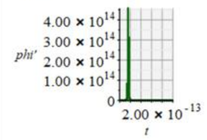

Figure 23

The particle can escape from the BH if its initial angular position is 90 degrees. For the remaining cases, the particle orbits the BH at a close distance and jumps away and back at 90-degree intervals in the polar direction, with very high velocity.

In Fig. 23 we have only one case of a particle escaping the black hole as shown on the third column of the table, for an angular initial position of $\theta = \frac{\pi}{2}$. In the first and fifth columns of the table it is shown how the particle hops away and back at 90-degree intervals in the polar direction, with extremely high velocity while orbiting the black hole at a close distance.

The second and fourth columns of the table show similar behaviors, with the particle orbiting between a maximum and minimum distance, and within a $\frac{\pi}{2}$ interval that is centered on the equatorial plane.

$r(0) = 10^5$ $[m]$ (~9.7 10^4 m away from the SR), $\dot{r}(0) = 10^2 \left[\frac{m}{s}\right]$ $\dot{\theta}(0) = 15 \left[\frac{rad}{s}\right]$ $\phi(0) = 0$ $[rad]$, $\dot{\phi}(0) = 10^{-9} \left[\frac{rad}{s}\right]$					
$\theta(0)$ $[rad]$	$\frac{\pi}{10^4}$ $(\theta \approx 0°)$	$\frac{\pi}{4}$	$\frac{\pi}{2}$	$\frac{3\pi}{4}$	π
$r(t)$ $[m]$	*Oscillatory. Particle does not reach the SR. Minimum approach distance* $r \approx 5.2\,10^3$ $[m]$	*Similar as for* $\frac{\pi}{10^4}$	*Same as for* $\frac{\pi}{10^4}$	*Same as for* $\frac{\pi}{4}$	*Same as for* $\frac{\pi}{10^4}$
$\dot{r}(t)$ $\left[\frac{m}{s}\right]$	*Oscillatory.* *Velocity peaks:* $v \approx \pm 1.7\,10^8 \left[\frac{m}{s}\right]$ *Distance vs. velocity (for* $t = 0..2\,10^{-2}\,s$*):* 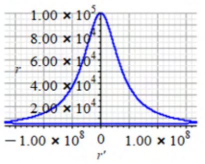	*Same as for* $\frac{\pi}{10^4}$	*Same as for* $\frac{\pi}{10^4}$	*Same as for* $\frac{\pi}{4}$	*Same as for* $\frac{\pi}{10^4}$
$\theta(t)$ $[rad]$	*Polar angle has jumps of* π*, switching between* 0*, and* π*. Polar graph of* $r(t)$ *vs* $\theta(t)$ *(for* $t = 0..2\,10^{-2}\,s$*).* 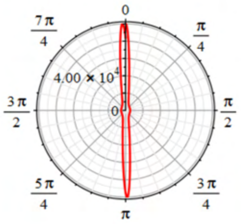	$\theta \approx \frac{\pi}{4}$	*Polar angle remains at* $\theta \approx \frac{\pi}{2}$ $[rad]$*. Polar graph of* $r(t)$ *vs* $\theta(t)$ *(for* $t = 0..5\,10^{-3}\,s$*).* 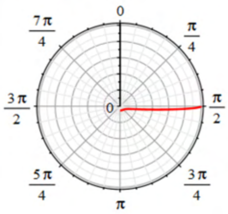	*Polar angle remains at* $\theta \approx \frac{3\pi}{4}$ $[rad]$*. Polar graph of* $r(t)$ *vs* $\theta(t)$ *(for* $t = 0..5\,10^{-3}\,s$*).* 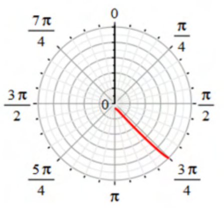	*Polar angle has jumps of* π*, switching between* 0*, and* π*. Polar graph of* $r(t)$ *vs* $\theta(t)$ *(for* $t = 0..10^{-2}\,s$*).* 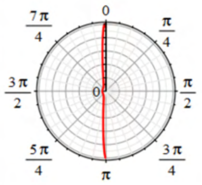
$\dot{\theta}(t)$ $\left[\frac{rad}{s}\right]$	*Polar angular velocity peaks with very high magnitudes* 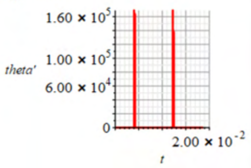	*Polar angular velocity peaks to high magnitude* 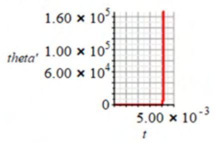	*Polar angular velocity peaks to high magnitude* 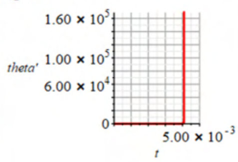	*Polar angular velocity peaks with high magnitude* 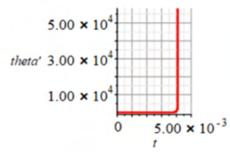	*Polar angular velocity peaks with very high magnitude* 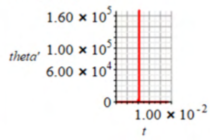
$\phi(t)$ $[rad]$	$\phi \approx 0$	$\phi \approx 0$	$\phi \approx 0$	$\phi \approx 0$	$\phi \approx 0$
$\dot{\phi}(t)$ $\left[\frac{rad}{s}\right]$	$\dot{\phi} \approx 0$	$\dot{\phi} \approx 0$	$\dot{\phi} \approx 0$	$\dot{\phi} \approx 0$	$\dot{\phi} \approx 0$

Figure 24

The particle never escapes from the BH. This case shows localized trajectories mainly along the rotational axis of the black hole with very high velocity.

We see in Fig. 24 that the particle never escapes from the black hole and exhibits localized trajectories along the rotational axis of the BH with very high velocity, as shown in the first and last columns of the table.

The table's other columns demonstrate how the particle orbit maintains its starting angular position when traveling at extremely high velocities away from the BH and back to a near distance without swinging to the opposite angle.

Summary of Particle Orbits Around a Black Hole

Even though the results are based on a small BH of $1M_{\odot}$, the analyzed motions will not be different for other BHs.

The new gravitational force law given by Eq. (5) is the only gravitational law that can clearly explain the origin of the so-called “astrophysical jets” around a black hole, as demonstrated by the results of the particle motion shown from Fig. (20) to Fig. (24).

The “astrophysical jets” are evident in several polar graphs of $r\ vs.\theta$ (in red) showing something similar to a bicycle wheel-like shape with no interlaced radial spokes, with **the jets distributed at discrete angles**. These jets are not only limited to polar directions. On Fig. 23 we also see polar graphs of $r\ vs.\phi$ (in green) showing that the same may happen in the azimuthal direction.

Thus, there is no need for other theories, such as the known Blandford–Znajek process, because the origin of high-energy particle beams is due to the electrodynamic interaction between a black hole and charged particles, as described by the newly derived gravitational law.

Additionally, it was shown in Fig. 20 the capture of particles by the BH for diverse initial conditions. The escape of particles from the BH is shown in columns 2, 3, and 4 of the table in Fig. 21.

A good example of particle escape is shown in column 3 of the table on Fig. 23, which is similar to the example we used to explain the so-called “velocity excess” on the outer arms of spiral galaxies. It is demonstrated how the particle reaches constant velocity after a certain time.

Also, we must not lose sight of the fact that in the new gravitational force given by Eq. (5), we replaced the original charges by the masses of the bodies to present the equation in a more “familiar” way with the lump Newtonian masses. However, **the interaction is indeed between the charges of the BH and the particle’s charge, not lump masses, and as such, it is an electrodynamic process.**

As a result, and due to the developed particle’s acceleration and velocity, we should expect radiation with extremely high magnitudes and incredible powerful magnetic fields that may extend far beyond the limits of the galaxy sustained by the black hole.

Conclusions

It has been proven that particle fusion is the electrodynamic origin of black holes, as definitely demonstrated by the universal electrodynamic total energy equation.

The universal shape of the curve of energy is clearly demonstrated by the total energy equation in particle fusion, black body radiation, binding energy per nucleon, and more.

It was demonstrated that particle velocity at the Schwarzschild radius is not limited to the speed of light as stated by the invalid and ill-fated theory of relativity.

The total energy equation also predicts a nucleus of small dimensions in black holes, where particles are trapped and energy absorption is much greater than energy release.

By applying the universal total energy equation, two derivations of the gravitational redshift have been made, providing more comprehensive equations with motion variables that are absent in the theory of relativity.

It has been established that a mathematical "singularity" does not exist at the center of a black hole; instead, there is a singular atom with minuscule dimensions, non-zero, and immense energy, yet not infinite, with a corresponding mass approximately 0.1% of the black hole's mass and a radiation temperature near absolute zero.

The estimated types of particles within and outside a black hole are described according to the new atomic theory. Their dimensions, total energy, potential energy, kinetic energy, and radiation energy are calculated for diverse radii within the black hole.

The radiation energy was used to calculate the radiating temperature and wavelength at different depths, demonstrating that Hawking radiation can never happen at the Schwarzschild radius but deep inside the nucleus of the black hole.

It is demonstrated that the cosmic background radiation is caused by electromagnetic waves of gravitational origin, as the radiation spectrum of an average black hole size is between microwaves and infrared, which is consistent with COBE NASA satellite measurements.

It was undeniably demonstrated that the new gravitational force is the sole gravitational law capable of elucidating the origin of the "astrophysical jets" surrounding black holes, as well as particle capture by black holes and particle escape from them.

Index

Bibliography

1. Raul Fattore, "Faster-Than-Light Travel Feasible with Negative Mass – Superluminal Dynamics", (2025)
2. Raul Fattore, "Nuclear Fusion Enhanced by Negative Mass – A Proposed Method and Device – (Part 3)", (2024)
3. Charles W. Lucas, Jr., "The Universal Electrodynamic Force" (2011), PROCEEDINGS of the NPA.
4. Raul Fattore, "Nuclear Fusion Enhanced by Negative Mass – A Proposed Method and Device – (Part 2)", (2024)
5. Raul Fattore, "New Atomic Model with Real-Valued Wave Function – Energy Levels, Spectrum, and Atomic Fine Structure", (2026)
6. A. K. T. Assis, "Gravitation as a Fourth Order Electromagnetic Effect", Advanced Electromagnetism: Foundations, Theory and Applications, T. W. Barrett and D. M. Grimes (eds.), (World Scientific, Singapore, 1995). https://www.ifi.unicamp.br/~assis/gravitation-4th-order-p314-331(1995).pdf
7. Charles W. Lucas, Jr. "The Electrodynamic Origin of the Force of Gravity", Part 1 (2008), Part 2 (2009), Part 3 (2009).
8. W. J. Hooper, "New Horizons in Electric, Magnetic, and Gravitational Field Theory", Electrodynamic Gravity, Inc., (1974)
9. N. Graneau, T. Phipps Jr, and D. Roscoe, "An experimental confirmation of longitudinal electrodynamic forces", The European Physical Journal, (2001)
10. Tifft, W. G. and Cocke, W. J., "Global Redshift Quantization", Astrophysical Journal, (1984).
11. Napier, W. M. and Guthrie, B. N. G., "Quantized Redshifts: A Status Report", Journal of Astrophysics and Astronomy, (1997).
12. Tifft, W. G., "Redshift Quantization in the Cosmic Background Rest Frame", Journal of Astrophysics and Astronomy, Volume 18, Issue 4, pp. 415-433, (1997).
13. Roscoe, D. F., "An Analysis of 900 Optical Rotation Curves", International Astronomical Union Symposium, 194, 379-383, (1999).
14. Duan, J.-L., Xiao, W., Guo, M., Liu, T., Chen, H. and Chen, J.-H., "Mimicking Symmetry-Breaking Einstein Ring by Optical Lens". Adv. Photonics Res., 6: 2400203. https://doi.org/10.1002/adpr.202400203, (2025).
15. Winston H. Bostick, "The Morphology of the Electron", International Journal of Fusion Energy, Vol. 3 No. 1, pp. 10-53 (1985), http://wlym.com/archive/fusion/ijfe/19850101-IJFE.pdf
16. S. W. Hawking, "Particle Creation by Black Holes", Communications in Mathematical Physics, (1975)
17. Raul Fattore, "Astronomical Distance Measurements Are Wrong – Galaxies Are Far Closer to Earth in Our Much Younger Universe", (2025)
18. Raul Fattore, "Full Free Motion of Celestial Bodies Around a Central Mass – Why Do They Mostly Orbit in the Equatorial Plane?", (2022)
